

Impact of Large-Scale Warming on Intraseasonal Variability of Indian Summer Monsoon Rainfall

Sumit Kumar Vishwakarma (✉ sumitvishwa8@gmail.com)

Indian Institute of Technology Kharagpur <https://orcid.org/0000-0001-5198-209X>

Research Article

Keywords: Indian Summer Monsoon Rainfall, Intraseasonal oscillation, Tropical Convergence Zone, Half a degree Additional warming Prognosis and Projected Impacts (HAPPI) experiment, Active and break period, Vertically Integrated Moisture Transport (VIMT)

Posted Date: January 19th, 2022

DOI: <https://doi.org/10.21203/rs.3.rs-1216632/v1>

License:  This work is licensed under a Creative Commons Attribution 4.0 International License.

[Read Full License](#)

Abstract

Indian summer monsoon, a part of the Asian summer monsoon is defined as the seasonal reversal of atmospheric circulation, is manifested in the form of northward migration of Inter-Tropical Convergence Zone (ITCZ) with respect to its normal position over the equator and resulting precipitation caused by the cross-equatorial moisture-laden south-westerly winds over the Indian subcontinent. Indian summer monsoon which is a complex geophysical phenomenon possesses a wide spectrum of variabilities such as daily, intraseasonal, interannual, decadal, and so on. The interaction between multiple modes of propagating intraseasonal oscillations of the Indian summer monsoon causes intermittent wet spells (i.e. active spells with good rainfall) and dry spells (i.e. breaks with little rainfall) over core monsoon zone. It is argued that a prolonged dry spells during July-August and an uneven temporal and spatial distribution of rains (even in normal monsoon years) has potential to have an adverse effect on agriculture. Therefore, understanding of the intraseasonal variation and the occurrence of the breaks, their intensity, and duration is very important. Indian summer monsoon region is vulnerable to global warming which is evident in the form of an increasing number of extremes and the increasing spatial variability of rainfall. The main focus of the study is to understand the nature of the break and characteristics of the break over all India monsoon regions and how active and break will vary with warming? This study investigates the impacts of warming on the core monsoon zone and all India monsoon regions by using the output of the 'Half a degree Additional warming Prognosis and Projected Impacts' (HAPPI) experiment model. There are five AGCM models are used in this study such as *NorESM1-HAPPI*, *ECHAM6.3-LR*, *CanAM4*, *MIROC5*, and, *CAM4-2degree*. Both, inter-model and intra-model comparisons are performed based on indicators such as the frequency and length of active and break spells for the historical period, plus15 period, and plus20 period (future). Vertically Integrated Moisture Transport (VIMT) pertaining to active and break is also analysed. An increase in moisture transport in the future active period under 1.5°C warming condition (plus15 future) and under 2°C warming condition (plus20 future) is expected in *NorESM1-HAPPI* model with intensification of rainfall over the core monsoon zone. Similarly, there will be intensification of breaks, and the core monsoon zone will receive less atmospheric moisture in future breaks under 1.5°C warming condition (plus15 future) and under 2°C warming condition (plus20 future).

Highlight

This study investigates the nature, characteristics and impacts of warming on the active and break spell over **Core Monsoon Zone** and **AIMR** by using the output of **(HAPPI)** experiment models such as ***NorESM1-HAPPI, ECHAM6.3-LR, CanAM4, MIROC5, and, CAM4-2degree***. Both, **inter-model** and **intra-model** comparisons are performed based on indicators such as the **frequency and length of active and break spells** for the historical period, plus15 period, and plus20 period (future). Vertically Integrated Moisture Transport **(VIMT)** pertaining to active and break is also analysed.

1.0 Introduction

1.1 Background

Indian summer monsoon, a part of the Asian summer monsoon is defined as the seasonal reversal of atmospheric circulation, is manifested in the form of northward migration of Inter-Tropical Convergence Zone (ITCZ) with respect to its normal position over the equator and resulting precipitation caused by the cross-equatorial moisture-laden south-westerly winds over the Indian subcontinent (Mohan et al., 2000). The Indian subcontinent receives 85% of its annual rainfall during the summer monsoon season which is crucial for fulfilling the demands of drinking water and agriculture. The importance of monsoon in the agricultural sector can be comprehended by a fact that more than 56% of the total agricultural land in India is rain-fed (Singh et al., 2014). Indian summer monsoon which is a complex geophysical phenomenon possesses a wide spectrum of variabilities such as daily, intraseasonal, interannual, decadal, and so on. The intrinsic spatial-temporal variabilities in the Indian monsoon system (also known as natural variabilities) is associated with the anomalies in the large-scale climate variables (which is mostly prominently) driven by the (temperature anomaly) (Bhatla and Ghosh, 2015). In particular, the intraseasonal variability of the Indian summer monsoon has a crucial role in deciding the fate of *kharif* crops in the Indian Subcontinent.

1.2 Intraseasonal variability of the Indian summer monsoon

The seasonal summer mean (June–September, JJAS) precipitation distribution over the Indian monsoon region has a major zone of large precipitation along the monsoon trough called low-pressure area extending from Northwest Rajasthan to the north Bay of Bengal (a core monsoon zone between 18-28° N and 73-82° E) and a secondary zone of precipitation maximum south of the equator (between 0° and 10°S) over the warm waters of the Indian Ocean. Locations of the Tropical Convergence Zone (TCZ) is represented by these two maxima during the summer monsoon season (Sikka and Gadgil 1980; Goswami 1994). The Intra-Seasonal Oscillations (ISOs) are fluctuations of the TCZ between these two locations and repeated propagation from the southern to the northern position within the monsoon season (Goswami and Ajaya Mohan, 2001). The interaction between multiple modes of propagating intraseasonal oscillations of the Indian summer monsoon causes intermittent wet spells (i.e. active spells with good rainfall) and dry spells (i.e. breaks with little rainfall) over core monsoon zone (Singh et al., 2013).

1.2.1 Definition of active and break spell1

‘Interval of droughts’ during which the large-scale rainfall over the monsoon zone is interrupted for several days in the peak monsoon months of July and August have been called breaks in the monsoon season. Active spells of the monsoon are the spells characterized by the ‘height of rains’ over the monsoon zone (Blanford 1886).

During a typical active condition, the northern TCZ is stronger and the southern one is weaker, with stronger cyclonic vorticity and enhanced convection over the northern location and stronger anticyclonic

vorticity and decreased convection over the southern one. During a typical break condition, this situation is reversed (Goswami and Ajaya Mohan, 2001).

Identifying for a break period, the criterion used by Indian meteorologists is the synoptic situation associated with rainfall anomaly, rather than the rainfall distribution itself. India Meteorological Department (IMD) generally defines breaks over the past several decades as the periods during which the monsoon trough (low-pressure area) is located close to the foothills of the Himalayas, which leads to a striking decrease of rainfall over most part of the country, but increase along the foothills of the Himalayas, southern peninsula and northeast part of the India (Mukhopadhyay et al., 2002).

Active and break spells are defined on the basis of the daily rainfall over the monsoon trough zone (low-pressure area) (Krishnan et al., 2000). A break spell is defined as the day on which the rainfall is below the specified thresholds and active spell, as the day on which the rainfall is above the specific threshold (Gadgil and Joseph, 2003).

A criteria suggested for identification of active and break events by using the high resolution daily gridded rainfall dataset over core monsoon zone (18-28° N and 73-82° E). If a period during which standardized rainfall anomaly is more than +1.0 consecutively for three or more days, it identified as an active period. Similarly, if a period during which the standardized rainfall anomaly is less than -1.0 consecutively for three or more days, it identified as a break period. It was observed that as compare to the active spells, breaks spells have longer life periods (Rajeevan et al., 2010).

It is argued that a prolonged dry spells during July-August substantially reduces crop yields. Furthermore, even in normal monsoon years an uneven temporal and spatial distribution of rains has an adverse effect on agriculture. Therefore, understanding of the intraseasonal variation and the occurrence of the breaks, their intensity, and duration is very important.

1.3 HAPPI experiment

The nations participated in Paris Agreement under the 'United Nations Framework Convention on Climate Change' (UNFCCC) set one goal for the protection of the climate under the long-term temperature change and the goal is to keep the global warming below 2°C and pursuing efforts to limit it below 1.5°C after the pre-industrial period, accepting that this would significantly reduce the impacts of climate change and risks under the warming scenario (Mitchell et al., 2017). It has been argued that low emission scenario such as 'Coupled Model Intercomparison Project phase five' (CMIP5) may not be best suited for achieving the goal of the Paris Agreement and also in scenario-based approach there was some uncertainty because of this limitation they designed one experiment which is called 'Half a degree Additional warming, Prognosis and Projected Impacts' (HAPPI) experiment. HAPPI experiment is a framework consisting of different models, which provides climatic datasets such as precipitation, wind speed, temperature, specific humidity and so on and describes how climate and extreme weather may different in present climate condition as compared to the 1.5°C and 2°C (future period) warming condition after the pre-industrial period (Mitchell et al., 2017).

1.4 Motivation

The Indian Summer Monsoon Rainfall (ISMR) possesses a large amount of variability in terms of its spatial distribution and seasonal strength especially since post-industrialization period after the 1950s (Roxy 2018). Asian summer monsoon region is most vulnerable to global warming due to frequent occurrence of events such as heavy precipitation, heat waves, and drought (Lee et al., 2018).

Recently, it has been observed that the global mean sea-surface temperature is increasing and it due to rapid warming of the western tropical Indian Ocean (Roxy et al., 2014), (Roxy 2018). Furthermore, the western Indian Ocean went through a great extent of warming of 1.28°C in summer SSTs as compare to the Indian Ocean which experienced an increase of 0.78°C during 1901-2012 (Roxy 2018). Western Indian Ocean which is generally cool in nature as compared to the tropical warm Ocean alters the zonal SST gradients and has the ability to change the circulation characteristics and rainfall of the Asian monsoon (Roxy 2018). The propagation and initiation of the Monsoon Intraseasonal Oscillation (MISO) are mainly governed by the ocean-atmospheric coupling of the Sea-Surface Temperature (SST), winds, convection and warming in the India ocean has an effect on its characteristics (Roxy 2018). The recent studies shows that as compared to the 1978-1988, northward-propagation characteristics of the MISO has changed during 2001-2011 due to the rapid increase in the SST temperature (Roxy 2018). Convection over the equatorial Indian Ocean is increased by the warming of the equatorial region which reduces the northward propagation of the MISO (Roxy 2018).

It is argued that, with respect to the pre-industrial period, an increase in 1.5°C global mean temperatures is projected to results in a 20% increase in daily rainfall, and under 2°C global mean temperature may results in a 25% increase in rainfall (Ali and Mishra, 2018).

At present, there is no study that focuses the impact of 1.5°C and 2°C warming on active and break spells in India, therefore, this study investigates the impacts of warming on the core monsoon zone and all India monsoon regions by using the output of the HAPPI experiment model. The purpose of this study is to provide detailed information of the future changes in active and break spells. The main focus of the study is to understand the nature of the break and characteristics of the break over all India monsoon regions under different target temperatures such as 1.5°C and 2°C and how active and break will vary with the warming?

1.5 Objectives

Keeping the above point in view, the present study has been planned with the following specific objectives for the study region. Based on the background and research gaps we have formulated the following sets of objectives.

1. To analyse the historical intraseasonal variability in HAPPI experiments.
2. To project active and break periods associated with rainfall variability for the future period.

3. To analyse the impact of warming on moisture transport.

2.0 Study Area And Data Availability

This section deals with the description of the study area Indian monsoon region with special emphasis on the core monsoon zone.

2.1 Study Area and Data

The extent of the present study mainly limited to the Indian Monsoon region and regions within its extent (i.e. Core monsoon zone (18-28° N and 73-82° E)). Rajeevan et al., (2010) identified that approximately 85% of the rainfall that occurs during the monsoon season over the core monsoon zone and the rainfall over core monsoon zone is considered as a representative of Indian monsoon signal, therefore we analyse the spatially averaged rainfall over the core monsoon zone.

In addition to that Pathak et al., (2014) and Pathak et al., (2017) found that the land-atmosphere interaction plays an important role in the precipitation process over this region. In addition to that, the land-surface feedback from this region not only fed the same region but also significantly contribute to the anomalous rainfall over the central part of India and north-east India. Therefore, in the present study, we analyse the role of large-scale warming on the intraseasonal variability over this region and over the core monsoon zone. Fig. 1 shows the geographic location of the core monsoon zone (represented with pink colour).

2.2. Data used

2.2.1 HAPPI datasets

National Energy Research Scientific Computing Center (NERSC) provides the output of the HAPPI experiment. We use five AGCMs models simulated datasets that participated in the HAPPI project (Table 1). These five AGCMs models have different physics and resolution therefore, we interpolated them to a common grid ($1^\circ \times 1^\circ$) resolution. Here, every member of five AGCM models provides 10-year simulated datasets for three periods.

i .Historical period (2006–2015) for the current decade

ii. Plus-15 (2106-2115) 1.5°C warming condition, for the future period

iii. Plus-20 (2106-2115) 2.0°C warming condition, for the future period

The key climate variables, such as precipitation (P), zonal wind (u wind), meridional wind (v wind), specific humidity (q) and surface pressure (ps) are used at a common resolution of ($1^\circ \times 1^\circ$) within the extent of latitude (-40°S to 54°N) and longitude (0°E to 360°W). A detailed information about the variable name, its dimension, pressure levels, and dimensions of the data is provided below.

a. Precipitation (P)(mm/day) 3D

- b. Specific Humidity (q)(kg/kg)(Pressure level 850,500,250 hPa) 4D
- c. Wind speed (ua & va)(m/sec)(Pressure level 850,500,250,100 hPa) 4D
- d. Surface pressure (ps)(Pa) 3D

Table 1
List of five AGCM used in this study.

Model name	Original horizontal resolution (longitude×latitude) (km×km)	No. of ensemble members
<i>CanAM4</i>	128 × 64	100
<i>CAM4-2degree</i>	144 × 96	500
<i>ECHAM6.3-LR</i>	192 × 96	100
<i>MIROC5</i>	256 × 128	100
<i>NorESM1-HAPPI</i>	288 × 192	125

2.2.2 Observed datasets

Daily gridded ($0.25^\circ \times 0.25^\circ$) precipitation datasets from IMD (Rajeevan et al., 2010) are used in this study for the historical period (2006-2015) over all India monsoon region with latitude ($8.25^\circ N$ to $37.25^\circ S$) & longitude ($68^\circ E$ to $97.25^\circ W$).

3.0 Materials And Methods

This chapter deals with the presentation of detailed theory and procedures. The organization of the section is as follows: Section 3.1 describe the flowchart of the workflow; Section 3.2 describes the multi criteria based selection; Section 3.3 describes the intraseasonal variability; Section 3.4 discusses vertically integrated moisture transport.

Figure 2 shows the flowchart of the methodology followed in this study. The tasks in the flowchart are divided into two parts intra-model comparison and intermodal comparison. In the present study as we are using five AGCM, not all AGCM have all the variables (except the precipitation) available at a common time resolution. Furthermore, it is observed that among, all the AGCM, the *NorESM1-HAPPI* model has almost all the required variables at the finer spatial and temporal scale. Thus a detailed intra-model comparison of intraseasonal precipitation variability is presented using the best runs of *NorESM1-HAPPI* model precipitation. Similarly, the inter-model comparison is also performed using the precipitation outputs from five different AGCM.

3.1 Intra-model comparison

The five AGCMs used in this study such as (i) *NorESM1-HAPPI* (ii) *ECHAM6.3-LR* (iii) *CanAM4* (iv) *MIROC5* and (v) *CAM4-2degree*. These five AGCM models are part of the HAPPI experiment which provides climatic data such as precipitation for the historical period, plus15 period, and plus20 period. Since, only *NorESM1-HAPPI* model has precipitation, specific humidity, wind vector, and air temperature data for the historical period, plus15 period and plus20 period as compared to the other four models used in this study, we select only *NorESM1-HAPPI* model for intra-model comparison (i.e. to identify the best run).

Figure 3 shows the deviation of long term All India Monsoon Rainfall (AIMR) climatology of ensembles (runs of the *NorESM1-HAPPI* Model) from the observed data (IMD). In Fig. 3, y-axis represents number of days (from 1 to 365) and x-axis represents ensembles runs (from 1 to 120). These ensemble runs are the simulated output of the *NorESM1-HAPPI* Model. Red colour represents higher deviation of the climatology from the observed data (IMD data) and blue colour represents lower deviation of the climatology from the observed data. It is clear from the Figure 3 that, there is lesser deviation is observed between pre-monsoon season and monsoon season. So we can select only those ensemble runs which have good performance during monsoon season. It is not clear from the Figure 3 that, which run we have to take, for furthermore analysis it is required to take best runs out of 120 runs.

Figure 4 shows the comparison between All India Monsoon Rainfall (AIMR) climatology of ensembles (runs of the *NorESM1-HAPPI* model), and observed precipitation (IMD data). The blue band represents observed range (obs. mean + 0.5S.D, obs. mean - 0.5S.D.) and the solid blue line represents observed mean climatology. Similarly, the orange band represents ensemble range (max of all runs, min of all runs) and the orange line represents mean of all runs. It is evident from Figure 4 that, all values of the ensemble values are slightly overestimated than that of observed climatology, however, they have a similar pattern of climatology. It is important to note that the ensemble mean has a lesser deviation than that of observed mean during the monsoon period, hence, we can pick some best runs out of entire ensembles. Thus, we have to select only those runs which are having better performance during the summer monsoon season (JJAS). Furthermore, in order to select the best runs from Fig. 4, further analysis is required to choose the best runs.

We use gridded observed precipitation data (from IMD Rajeevan et al., 2010), to identify the best runs within the *NorESM1-HAPPI* datasets. The best runs were identified based on multi-criteria such as *RCAAnMax*, *RCMSE*, *RCRMS*, *RCCMZCorr*, *RCRXAday*, *RCR95P*, and *RCRX5day*. It is important to note that, these criteria are based on different statistics and each of these criteria provides one best run. Seven out of 120 runs were identified as the best runs within the *NorESM1-HAPPI* datasets and thus used for analysing intraseasonal variability such as active and break period.

3.1.1 Selection Criteria

RCAAnMax (*Ability of model to simulate long term annual maximum*): This criterion is used to capture interannual variability of rainfall over the all India monsoon region. First, the maximum of each year is

calculated which is called annual maximum after that, average of the maximum value is calculated then we compared with the observed value, whichever run value was near to the observed value, a highest rank was assigned to that run.

RCMSE (Mean square error of daily precipitation): This criterion is used to capture the daily variability of all India monsoon rainfall. First, mean square error of both observed data and model data are calculated then deviation from the observed data is calculated, whichever run value was near to the observed value, a highest rank was given to that run. Mean square error is calculated by the following formula (1).

$$MSE = \frac{1}{n} \sum_{i=1}^n (Y_{oi} - Y_{mi})^2 \quad (1)$$

where, Y_{oi} = observed rainfall data

Y_{mi} = model rainfall data

n = total no. of data

RCRMS (Root mean square of daily precipitation):- This criterion is used to capture the daily variability of all India monsoon rainfall. First, the root means square of both observed data and model data are calculated then deviation from the observed data is calculated, whichever run value was near to the observed value, a highest rank was given to that run. Root mean square is calculated by the following formula (2).

$$RMS = \sqrt{\frac{\sum_{i=1}^n (Y_{oi} - Y_{mi})^2}{n}} \quad (2)$$

where, Y_{oi} = observed rainfall data

Y_{mi} = model rainfall data

n = total no. of data

RCCMZCorr (Correlation of JJAS daily precipitation of core monsoon zone): This criterion is used to capture grid wise seasonal variability of core monsoon zone rainfall. First, the correlation coefficient of both the observed data and model data is calculated then deviation from the observed data is calculated, whichever run value was near to the observed value, a highest rank was assigned to that run. Correlation coefficient is calculated by the following formula (3). (Rajeevan et al., 2010)

$$r = \frac{\sum_{i=1}^n (X_i - \bar{X})(Y_i - \bar{Y})}{\sqrt{\sum_{i=1}^n (X_i - \bar{X})^2} \sqrt{\sum_{i=1}^n (Y_i - \bar{Y})^2}}$$

3

where, X_i = observed rainfall dataset

\bar{X} = mean of observed rainfall

X_i = observed rainfall dataset

Y_i = Model rainfall dataset

\bar{Y} = mean of model rainfall

r = Correlation coefficient

Figure 5 shows the correlation between the core monsoon zone and rainfall over all India nodes in IMD and *run060*. Pink color shows the minimum value of the correlation coefficient and dark purple color shows the maximum value of the correlation coefficient. Maximum correlation coefficient is observed over the core monsoon zone. Therefore, we can confirm that there is a good correlation between observed data and *run060*. So we are selecting run number 060 because it shows a good correlation with observed data.

RCRXAday (Skill score of JJAS daily precipitation): This criterion is used to capture the daily variability of all India monsoon rainfall. First, the probability distribution of both the observed and model data is calculated for a given bin then the cumulative minimum value of the observed and model data is calculated which is called skill score value (Change and Frontiers, 2007). Whichever runs skill score value is observed maximum that run is given the highest rank. If a model simulates observed condition perfectly it will have a skill score is equal to one, it means that there is a perfect overlap between the observed data and model data. If a model simulates observed condition poorly it will have zero skill score with negligible overlap between the observed data and model data. S score is calculated by the following equation (4). (Perkins et al., 2007)

$$Sscore = \sum_1^n \min(Z_m, Z_o) \quad (4)$$

Where, n = no. of bins used to calculate Probability Density Function (PDF)

Z_m = Probability of model data in a given bin

Z_o = Probability of observed data in a given bin

Figure 6 shows the comparison of skill score between observed data and run078. In this figure, the y-axis represents the probability, and the x-axis represents precipitation in mm/day. Blue colour histogram represents observed value and orange colour histogram represents run078 value. Maroon colour histogram represents overlapping between observed data and run078. The graph shows that there is a 74% overlap between observed data and run078. So we are selecting *run 078* because it shows the good overlap with the observed data.

RCR95P (Annual JJAS daily precipitation > 95th percentile of JJAS wet days): This criterion is used to capture spatial and extreme variability of all India monsoon rainfall. Wet days are defined as the annual count of JJAS days when daily precipitation is ≥ 1 mm/day. Ninety-five percentile of JJAS wet days is calculated and we are taken only that value of annual JJAS daily precipitation whose value is greater than 95 percentile of wet days, similarly for the observed datasets. After that, we calculated the skill score for both the observed data and model data. Whichever runs skill score value is maximum that run is given the highest rank. (Diaconescu et al., 2017)

RCRX5Day (Annual JJAS maximum of 5-day accumulated precipitation): This criterion is used to capture the spatial variability of all India monsoon rainfall. Five-day accumulated precipitation is calculated by the moving average method. From the five-day accumulated precipitation, we are taken the annual maximum of each JJAS, similarly for the observed datasets. After that, we calculated the skill score for both the observed data and model data. Whoever skill score value was maximum that value is given the highest rank. (Diaconescu et al., 2017)

Table 2
Criteria-wise best runs.

Sr. No.	Criteria Code	Description	Formula	Run No.
1	<i>RCAAnMax</i>	Long term annual maximum		052
2	<i>RCRX5Day</i>	JJAS max of 5-day accumulated precipitation	$Sscore = \sum_1^n \min(Z_m, Z_o)$	056
3	<i>RCCMZCorr</i>	Correlation of JJAS daily precipitation of CMZ	$r = \frac{\sum_{i=1}^n (X_i - \bar{X})(Y_i - \bar{Y})}{\sqrt{\sum_{i=1}^n (X_i - \bar{X})^2} \sqrt{\sum_{i=1}^n (Y_i - \bar{Y})^2}}$	060
4	<i>RCR95P</i>	Annual JJAS precipitation > 95th percentile	$Sscore = \sum_1^n \min(Z_m, Z_o)$	070
5	<i>RCRMS</i>	Root mean square of daily precipitation	$RMS = \sqrt{\frac{\sum_{i=1}^n (Y_{oi} - Y_{mi})^2}{n}}$	073
6	<i>RCMSE</i>	Mean square error of daily precipitation	$MSE = \frac{1}{n} \sum_{i=1}^n (Y_{oi} - Y_{mi})^2$	074
7	<i>RCRXADay</i>	S score of JJAS daily precipitation	$Sscore = \sum_1^n \min(Z_m, Z_o)$	078

Figure 7 shows the selection of the best runs based on different criteria. In this figure, the rows represents seven criteria and the column represents runs. The value represented with red colour shows the highest rank (minimum value) and shades of grey colour shows the rank for each of these criteria. It is clearly visible from the graph that for *RCAAnMax*, *RCRX5Day*, *RCCMZCorr*, *RCR95P*, *RCRMS*, *RCMSE*, and *RCRXADay* criteria, *run052*, *run056*, *run060*, *run070*, *run073*, *run074*, and *run078* is the best run. This is also summarized in Table 2.

3.2 Inter-Model comparison of the intraseasonal variability:

For further investigation of the intraseasonal variability, we consider all five AGCM model. Five AGCM (*NorESM1-HAPPI*, *ECHAM6.3-LR*, *CanAM4*, *MIROC5*, and *CAM4-2degree*) models that are the part of the HAPPI experiment which provides precipitation data for the historical period, plus15 period and plus20 period area selected. The performance of each of these AGCMs in terms of historical climatology is tested with respect to the observed data (IMD). All five AGCM models interpolated at a common grid (1°×1°) resolution in order to compare their performance. Intraseasonal variability such as active and break spells of all the five AGCM models are calculated for the historical period, plus15 period, and plus20 period.

Figure 8 shows the comparison between Core Monsoon Zone (CMZ) rainfall climatology of ensembles (runs of five AGCM models) and observed rainfall (IMD data) during historical period. The blue band

represents observed range (obs. mean + 0.5S.D, obs. mean - 0.5S.D.) and the solid blue line represents observed mean climatology. Similarly, the black band represents ensemble range (values of all runs) of *NorESM1-HAPPI* Model and the black line represents mean of all runs of *NorESM1-HAPPI* Model. The red band represents ensemble range (values of all runs) of *MIROC5* Model and the red line represents mean of all runs of *MIROC5* Model. In a similar way, the pink band represents ensemble range (values of all runs) of *CanAM4* Model and the pink line represents mean of all runs of *CanAM4* Model. Likewise, the green band represents ensemble range (values of all runs) of *CAM4-2degree* Model and the green line represents mean of all runs of *CAM4-2degree* Model. In a similar manner the orange band represents ensemble range (values of all runs) of *ECHAM6-3LR* Model and the orange line represents mean of all runs of *ECHAM6-3LR* Model. It is clear from Figure 8 that, all values of the ensembles values of *MIROC5* Model are slightly overestimated than that of the observed climatology. Ensembles of the *NorESM1-HAPPI* Model, *CanAM4* Model, *CAM4-2degree* Model and *ECHAM6-3LR* Model shows a similar pattern of climatology than that of the observed data. It is clear from the Figure 8 that *MIROC5* Model is not good whereas *NorESM1-HAPPI* Model, *CanAM4* Model, *CAM4-2degree* Model and *ECHAM6-3LR* Model are good. So for further analysis we can choose only these Models such as *NorESM1-HAPPI*, *CanAM4*, *CAM4-2degree* and *ECHAM6-3LR*.

3.3 Characteristics of active and break spells

Intraseasonal variability of ISMR in terms of active and break spells is studied for the historical period, plus15 period, and plus20 period. Key characteristics of Active and Break spells are given below.

3.3.1 Active spells:

- Good rainfall over the Core monsoon region
- Rainfall 1 to 4 times of the normal rainfall
- Enhanced rainfall activity over central India
- Wind speed 23 to 32 knots over the sea
- Increased low-level cyclonic vorticity over northern tropical convergence zone and reduced low-level cyclonic vorticity over southern tropical convergence zone
- Increased convection over northern tropical convergence zone and reduced convection over southern tropical convergence zone
- Negative outgoing longwave radiation anomaly

3.3.2 Break Spells:

- Little or no rainfall over the Core monsoon zone
- Rainfall is less than half of the normal rainfall
- Rainfall activity mainly concentrated near foothills of Himalayan, North-east parts of India and southern peninsula
- Wind speed 12 knots over the sea

- Decreased low level cyclonic over northern tropical convergence zone and enhanced low-level cyclonic vorticity over southern tropical convergence zone
- Decreased convection over northern tropical convergence zone and enhanced convection over southern tropical convergence zone
- Positive outgoing longwave radiation anomaly

3.3.3 Length of active and break spells:

Length of the active and break spells are calculated by the daily gridded rainfall dataset over the core monsoon zone (18-28° N and 73-82° E) (M. Rajeevan et al., 2010). It is calculated by taking the average of daily rainfall and standardizing the daily rainfall time series by subtracting from its long term normal mean and by dividing with its daily standard deviation over the core monsoon zone. If the periods during which standardized rainfall anomaly is more than ± 1.0 consecutively for three or more days identified as an active period. Similarly, if the periods during which the standardized rainfall anomaly is less than -1.0 consecutively for three or more days identified as a break period.

3.3.4 Frequency of active and break spells:

Frequency of active and break spells is calculated by the number of times active and break events occurring in each year.

3.4 Vertically Integrated Moisture Transport (VIMT)

Moisture transport is an essential process of the earth's hydrological cycle (Sinha et al., 2019). Vertically integrated moisture transport is directly associated with the monsoon rainfalls. For ISMR at a global scale, different moisture source regions are identified by Pathak et al., (2016) and Stohl and James, (2004, 2005). Pathak et al., (2016) identified key moisture source regions such as the western Indian Ocean, the central Indian Ocean, the upper Indian Ocean (that includes Bay of Bengal) and the Ganga Basin (recycling). For monsoon rainfall over western and southern India, four major source regions are identified by the Ordóñez et al., (2012) such as Arabian Sea, the Indian Ocean (through the Somali low-level jet), the north-western part of the Indian subcontinent, western and southern India (through evapotranspiration) and the Bay of Bengal during the winter season. During the summer monsoon season, moisture is transported from the Arabian Sea and Bay of Bengal over the Indian region and subcontinent (Pathak et al., 2017),(Ullah and Gao, 2012). The Bay of Bengal possesses some special characteristics such as it has relatively high sea surface temperature, as compared to the other Indian Ocean during the monsoon season (Sinha et al., 2019). Northern Bay of Bengal represents the genesis of the low-pressure systems (LPS) and moves towards the western part of the India and creates heavy rainfall over the central and northern India (Goswami 1994). Contribution of moisture transport from the Arabian Sea and Bay of Bengal to the Indian monsoon rainfall is to be highly modulated at intraseasonal time scales (Pathak et al., 2017). Thus, sources of moisture transport from the local oceanic sources, over the core monsoon zone on intraseasonal time scales is very important to understating the intraseasonal variability of the monsoon as well as seasonal mean monsoon (Sinha et al., 2019). Vertically integrated moisture transport is calculated by the equation 5 (Ullah and Gao, 2012).

$$VIMT = \frac{1}{g} \int_0^{ps} (qU) dp$$

5

where,

VIMT = vertically integrated moisture transport in (*kg m/sec*)

ps = pressure at different pressure levels (250, 500, 750 *hPa*)

U = resultant of zonal (*u wind*) and meridional (*v wind*) wind vector at different pressure levels (250, 500, 750 *hPa*) in *m/sec*

q = specific humidity at different pressure levels (250, 500, 750 *hPa*) in *kg/kg*

g = gravitational acceleration in (*9.81 m/sec²*)

Changes in the precipitation is calculated by the equation 6

$$\delta(\cdot) = (\cdot)Plus - (\cdot)HIST$$

6

where,

$\delta(\cdot)$ = Difference between future period and historical period

$(\cdot)Plus$ = datasets for plus15 and plus20 periods

$(\cdot)HIST$ = datasets for the historical period.

4.0 Results And Discussion

This section discusses the findings in two parts. First one is the results of criteria based selection of the *NorESN1-HAPPI* model for intra-model comparison and second one is the inter-model comparison of the intraseasonal variability in five AGCM models.

4.1 Intra-model comparison for the historical period

4.1.1 Length of active and break period

Figure 9 shows the length of the active and break period of the selected best runs. The length of the active period (in red colour boxplot) and break period (in blue colour boxplot) shown for different criteria. The outliers present in the datasets are indicated by a plus (+) symbol. It is observed that the minimum length of active and break period is three days and the maximum length of active days is 10 days and the maximum length of break days is 11 days during the historical period. Break periods have a higher length

than the active periods. Long intense breaks are often associated with poor monsoon rainfall over the core monsoon zone and central India and have a large impact on rainfed agriculture.

4.1.2 Frequency of active and break period

Frequency of active and break spells is calculated by the number of times active and break events occur in each year. Generally, a higher number of the frequency of active days means a more intense rainfall and more frequent moisture over the core monsoon zone and central India.

Figure 10 shows the comparison between the frequency of the active period for the selected runs of *NorESM1-HAPPI* and the observed IMD data. Minimum frequency of the active period is zero days and the maximum frequency of the active period is ten days. It is evident from Figure 10 that the frequency of *RCRXADay* is close to the observed data (IMD rainfall).

Figure 12 shows the comparison between the frequency of the break period for selected runs of *NorESM1-HAPPI* and the observed IMD data. It is observed that the minimum frequency of the break period is zero days and the maximum frequency of the break period is five days. It is evident from Figure 12 that the frequency of *RCRX5Day* and *RCMSE* is close to the observed data (IMD rainfall). Thus, the *RCRX5Day* and *RCMSE* are able to reflect the observed variations in the break period during the historical period.

4.1.3 Distribution of the active and break duration and associated probability

Figure 13 shows the distribution of the active period duration and the associated probability. Among all active events, periods with duration equals to 3-4 days and 4-5 days have a high probability than that of the >7 days duration active periods. There is a high probability for events with duration equals 3-4 days, in case of *RCRXADay* run has a maximum probability of 3-4 days, 4-5 days in case of *RCCMZCorr*. Among all the runs the highest probability of 5-6 days, 6-7 days, 7-8 days, 8-9 days, and 9-10 days is observed in the case of the *RCAAnMax*, *RCR95*, *RCMSE*, *RCRX5Day*, and *RCRX5Day* runs respectively.

Figure 14 shows the distribution of the break duration and associated probability. Among all the break events, periods with duration equals to 3-4 days and 4-5 days have a high probability than that of the >7 days duration break periods. There is a high probability for events with duration equals 3-4 days in case of *RCRXADay* run and 4-5 days in case of *RCAAnMax* criteria run. Among all the runs the highest probability of 5-6 days, 6-7 days, 7-8 days, 8-9 days, 9-10 days, and 10-11 days is observed in the case of the *RCRX5Day*, *RCR95*, *RCRXADay*, *RCRMS*, *RCRMS*, and *RCRMS* runs respectively

4.2 Inter-model comparison of the intraseasonal variability

4.2.1 Length of the active period during historical, plus15 and plus20 period

A two-sample *t-test* is performed to test the significance of the observed change in length of the active period between the historical and future periods (plus15 and plus20). We take the null hypothesis that the two data samples come from independent random samples from normal distributions with equal means and equal but unknown variances.

Where, *p-value* = probability of the distribution.

$h = 1$, this indicates the rejection of the null hypothesis at 5% significance level.

$h = 0$, this indicates a failure to reject the null hypothesis at 5% significance level.

Table 3 shows the results of a two-sample *t-test* for the historical period and plus15 period. In this table, the value of $h = 1$, represents a rejection of the null- hypothesis, and significance for that model and the value of $h = 0$, indicates a failure to the reject null-hypothesis and non-significance for that model. The models *ECHAM6.3-LR*, *MIROC5*, and *NorESM1-HAPPI* show a significant change in length of the active period, and for the rest of the models change is not significant. For further analysis of the length of the active period, we are considering only these models *ECHAM6.3-LR*, *MIROC5*, and *NorESM1-HAPPI*.

Table 3
t-test of the length of the active period between historical and plus15 period.

Model name	h value (hist. and plus15)	p-value (hist. and plus15)
<i>CanAM4</i>	0	0.6413
<i>ECHAM6.3-LR</i>	1	0.0181
<i>CAM4-2degree</i>	0	0.2887
<i>MIROC5</i>	1	0.0122
<i>NorESM1-HAPPI</i>	1	1.28e-08

Table 4 shows the results of a two-sample *t-test* for the length of the active period between the historical period and plus20 period for five AGCM models. The models *ECHAM6.3-LR*, *CAM4-2degree*, *MIROC5*, and *NorESM1-HAPPI* show a significant change in length of the active period, and for the rest of the models change is not significant. For further analysis of the length of the active period, we are considering only these models *ECHAM6.3-LR*, *CAM4-2degree*, *MIROC5*, and *NorESM1-HAPPI*.

Table 4

t-test of the length of the active period between historical and plus20 period.

Model name	h value (hist. and plus20)	p-value (hist. and plus20)
<i>CanAM4</i>	0	0.1027
<i>ECHAM6.3-LR</i>	1	0.0305
<i>CAM4-2degree</i>	1	0.0427
<i>MIROC5</i>	1	0.0020
<i>NorESM1-HAPPI</i>	1	1.57e-129

Figure 15 shows the length of the active period between historical, plus15 (future), and plus20 (future). Black solid line represents mean, red solid line represents median, and blue solid line represents the 95th percentile of the data. *ECHAM6.3-LR* model shows the mean active length of the active period is four days with no changes between historical, plus15, and plus20 period. In *ECHAM6.3-LR* and *MIROC5* models, although there is no change in mean active length, the probability density of active period duration is slightly changed with a few long duration active periods in the future period. Similarly, in case of a *CAM4-2degree* model, mean active length is unchanged, however, the range of durations is slightly reduced for the future period. *NorESM1-HAPPI* model, shows slightly increased in mean length of active period for plus20 future period, and also there is a slightly elongated probability density of active period durations for the future period. An increase in the length of the active period will result into more moisture during the plus20 future period than that of the historical period over the India and subcontinent region. There will be more rainfall over India and subcontinent region in future under 2°C warming condition.

4.2.2 Length of break period between historical plus15 and plus20 period

Table 5 shows the results of a two-sample *t*-test between the length of the break period for the historical period and plus15 period for five AGCM models. The models *CanAM4*, *CAM4-2degree*, and *NorESM1-HAPPI* show a significant change in length of break period, and for the rest of the models change is not significant. For further analysis of the length of the break period, we are considering only these models *CanAM4*, *CAM4-2degree*, and *NorESM1-HAPPI*.

Table 5
t-test of the length of break period between historical and plus15 period.

Model name	h value (hist. and plus15)	p-value (hist. and plus15)
<i>CanAM4</i>	1	6.71e-11
<i>ECHAM6.3-LR</i>	0	0.7575
<i>CAM4-2degree</i>	1	2.93e-05
<i>MIROC5</i>	0	0.2279
<i>NorESM1-HAPPI</i>	1	1.06e-06

Table 6 lists the results of a two-sample *t-test* between the length of the break period for the historical period and the plus20 period for five AGCM models. The models *CanAM4*, *CAM4-2degree*, and *NorESM1-HAPPI* show a significant change in length of break period, and for the rest of the models, change is not significant. For further analysis of the length of the break period, we are considering only these models *CanAM4*, *CAM4-2degree*, and *NorESM1-HAPPI*.

Table 6
t-test of the length of break period between historical and plus20 period.

Model name	h value (hist. and plus20)	p-value (hist. and plus20)
<i>CanAM4</i>	1	2.72e-11
<i>ECHAM6.3-LR</i>	0	0.4920
<i>CAM4-2degree</i>	1	3.54e-06
<i>MIROC5</i>	0	0.8312
<i>NorESM1-HAPPI</i>	1	1.50e-13

Figure 16 shows the length of the break period between historical, plus15 (future), and plus20 (future). Black solid line represents mean, red solid line represents the median, and the blue solid line represents the 95th percentile of the data. All the model shows the minimum length of the break period is three days. *CanAM4* model shows the mean length of break period is six days for historical and eight days for plus15 and plus20 period, as compared to the historical period there is slightly increased in length of break period in the future period. *CAM4-2degree* model shows, there is no change in the mean length of the break period for the future but the probability density is slightly changed with few long-duration break periods in the future than the historical period. *NorESM1-HAPPI* model shows, there is slightly increased in mean length of break period for plus20 future period and there is no change in mean length of break period for plus15 future than the historical period and also there are few additional long-duration break periods expected in the future period. An increase in the length of the break period in the future will reduce moisture than that of the historical period over the India and subcontinent region in the future. There will be relatively less rainfall over India and subcontinent region in the future. So we can store a definite amount of water from the active period which will be used during the break period. Therefore, we will

have to plan our irrigation system and agricultural activity accordingly towards a sustainable future period.

4.2.3 Frequency of active period between historical plus15 and plus20 period

Table 7 shows the results of a two-sample *t-test* between the frequency of the active period for the historical period and the plus15 period for five AGCM models. All five models are significant. For further analysis of the frequency of the active period, we are considering all the five models.

Table 7
t-test of the frequency of the active period between historical and plus15 period.

Model name	h value (hist. and plus15)	p-value (hist. and plus15)
<i>CanAM4</i>	1	2.78e-14
<i>ECHAM6.3-LR</i>	1	1.21e-07
<i>CAM4-2degree</i>	1	1.00e-07
<i>MIROC5</i>	1	1.83e-31
<i>NorESM1-HAPPI</i>	1	1.10e-07

Table 8 shows the results of a two-sample *t-test* between the frequency of the active period for the historical period and the plus20 period for five AGCM models. The models *CanAM4*, *ECHAM6.3-LR*, *CAM4-2degree*, and *NorESM1-HAPPI* show a significant change in length of the active period, and for the rest of the models change is not significant. For further analysis of the length of the active period, we are considering only these models *CanAM4*, *ECHAM6.3-LR*, *CAM4-2degree*, and *NorESM1-HAPPI*.

Table 8
t-test of the frequency of the active period between historical and plus20 period.

Model name	h value (hist. and plus20)	p-value (hist. and plus20)
<i>CanAM4</i>	1	1.10e-20
<i>ECHAM6.3-LR</i>	1	5.20e-12
<i>CAM4-2degree</i>	1	3.37e-09
<i>MIROC5</i>	0	0.4770
<i>NorESM1-HAPPI</i>	1	1.03e-209

Figure 17 shows the frequency of active period between historical, plus15 (future), and plus20 (future). *CanAM4* and *MIROC5* model show a slight increase in the mean frequency of active period (by 1 event) in plus15 and plus20 period. *CAM4-2degree* and *ECHAM6.3-LR* model shows a slight increase in the mean frequency of active period (by 1 event) for the plus20 period, however, it is slightly increased in the case

of *CAM4-2degree* model for plus15 future period. Furthermore, the *NorESM1-HAPPI* model shows the mean frequency of the active period is three events for historical and five events for plus15 and plus20 period. An increase in the average number of active days and intensity is observed towards the future period which indicates the possibility of more frequent wet days in the future. It will bring more frequent moisture in future periods than that of the historical period and there will be more intense rainfall in the future period over the core monsoon zone and central India.

4.2.4 Frequency of break period between historical plus15 and plus20 period

Table 9 shows the results of a two-sample *t-test* between the frequency of the break period for the historical period and plus15 period for five AGCM models. All five models are significant. For further analysis of the frequency of the active period, we are considering all the five models.

Table 9
t-test of the frequency of the break period between historical and plus15 period.

Model name	h value (hist. and plus15)	p-value (hist. and plus15)
<i>CanAM4</i>	1	7.83e-05
<i>ECHAM6.3-LR</i>	1	0.0002472
<i>CAM4-2degree</i>	1	1.099e-19
<i>MIROC5</i>	1	0.00114847
<i>NorESM1-HAPPI</i>	1	1.465e-26

Table 10 shows the results of a two-sample *t-test* between the frequency of the break period for the historical period and the plus20 period for five AGCM models. The models *CanAM4*, *ECHAM6.3-LR*, *CAM4-2degree*, and *NorESM1-HAPPI* show significant in the frequency of active period, and the rest of the models are not significant. For further analysis of the frequency of the active period, we are considering only these models *CanAM4*, *ECHAM6.3-LR*, *CAM4-2degree*, and *NorESM1-HAPPI*.

Table 10
t-test of the frequency of the break period between historical and plus20 period.

Model name	h value (hist. and plus20)	p-value (hist. and plus20)
<i>CanAM4</i>	1	3.5265e-05
<i>ECHAM6.3-LR</i>	1	0.0257710
<i>CAM4-2degree</i>	1	3.2995e-23
<i>MIROC5</i>	0	0.8515636
<i>NorESM1-HAPPI</i>	1	8.6954e-15

Figure 18 shows the frequency of the break period between historical, plus15 (future), and plus20 (future). *CanAM4* model shows a slightly increased (by 1 event) the mean frequency of break period in plus15 and plus20 period, whereas the *ECHAM6.3-LR* model the mean frequency is increased by three events for plus15 period and two events for plus20 period. The mean frequency of the active period is slightly increased in the plus15 period (by 1 event), and plus20 period (by 2 events) in case of the *CAM4-2degree* model. *MIROC5* model also shows a slight increase in mean frequency of break period (by 1 event) for plus15 period than during the historical period. *NorESM1-HAPPI* model shows the mean frequency of break period is two events for historical, three events for plus15 and two events for plus20 period, hence as compared to the historical period there is slightly increased in frequency of break period in the future period. An increase in the average number of break days and intensity is observed towards the future period. It may be reduce moisture transport from the local oceanic sources towards the future period. There will be relatively less rainfall over India and subcontinent region in the future due to the enhancement of breaks. It will create drought-like situations and adversely affect the agriculture sector of the country for which proper irrigation plans and policies may be planned towards the future.

4.3 Active and break period of the *CanAM4* model under 1.5°C and 2°C warming condition

4.3.1 Active and break period of the *CanAM4* model for historical and plus15 period

Figure 19 shows the rainfall during the active and break period of the *CanAM4* model for historical and plus15 period. Active period has increased amount of rainfall over the core monsoon zone and decreased amount of rainfall over the North-east part of the India, in plus15 future period as compared to the historical period. During plus15 (future) breaks, there is an increased amount of rainfall over the North-east part of the India and less rainfall over the core monsoon zone. We may expect an intensification of the break period in the plus15 future period.

4.3.2 Active and break period of the *CanAM4* model for historical and plus20 period

Figure 20 shows the rainfall during the active and break period of the *CanAM4* model for historical and plus20 period. Active periods have increased amount of rainfall over the core monsoon zone and decreased amount of rainfall over the North-east part of the India, in plus20 future period as compared to the historical period. During plus20 (future) breaks, there is an increased amount of rainfall over the North-east part of the India and less rainfall over the core monsoon zone. Here, also we may expect an intensification of the break period in the plus20 (future) period.

4.4 Active and break period of the *ECHAM6-3LR* model under 1.5°C and 2°C warming condition

4.4.1 Active and break period of the *ECHAM6-3LR* model for historical and plus15 period

Figure 21 shows the rainfall during the active and break period of the *ECHAM6-3LR* model for historical and plus15 period. It is important to note that there is no rainfall data/missing values over the ocean, hence the values do not reflect the actual change. Active period has slightly increased amount of rainfall over the core monsoon zone and central India and decreased amount of rainfall over the North-east part of the India and southern peninsula, in plus15 (future) period as compared to the historical period. During plus15 (future) breaks, there is a slightly increased amount of rainfall over the North-east part of the India and southern peninsula and less rainfall over the core monsoon zone. Here, as well, we may expect an intensification of the break period in plus15 future period.

4.4.2 Active and break period of the *ECHAM6-3LR* model for historical and plus20 period

Figure 22 shows the rainfall during the active and break period of the *ECHAM6-3LR* model for the historical and plus20 period and also shows that there is no rainfall data for the *ECHAM6-3LR* model over the ocean. Active period has slightly increased amount of rainfall over the core monsoon zone and decreased amount of rainfall over the North-east part of the India, in plus20 future period as compared to the historical period. During plus20 (future) breaks, there is an increased amount of rainfall over the southern peninsula and less rainfall over the core monsoon zone. We may expect an intensification of the break period in the plus20 future period.

4.5 Active and break period of the *CAM4-2degree* model under 1.5°C and 2°C warming condition

4.5.1 Active and break period of the *CAM4-2degree* model for historical and plus15 period

Figure 23 shows the rainfall during the active and break period of the *CAM4-2degree* model for historical and plus15 period. We may expect a significant change in core monsoon zone rainfall during the active period, however slightly increased in rainfall near the southern part of the India is expected as per the results from the *CAM4-2degree* model. During plus15 (future) breaks, there is an increased amount of rainfall over the North-east part of the India and less rainfall over the core monsoon zone, and hence, we may expect an intensification of the break period in plus15 future period.

4.5.2 Active and break period of the *CAM4-2degree* model for historical and plus20 period

Fig. 24 shows the rainfall during the active and break period of the *CAM4-2degree* model for the historical and plus20 period. A slight increase in rainfall is expected over the core monsoon zone and central India in plus20 active period. During plus20 (future) breaks, there is an increased amount of

rainfall over the North-east part of the India and near the foothills of the Himalayan region and almost no change in rainfall over the core monsoon zone. The equatorial convergence zone which normally receives more rainfall during the break, may receive less rainfall in plus20 future.

4.6 Active and break period of the *MIROC5* model under 1.5°C and 2°C warming condition

4.6.1 Active and break period of the *MIROC5* model for historical and plus15 period

Figure 25 shows the rainfall during the active and break period of the *MIROC5* model for historical and plus15 period. The core monsoon zone will receive a surplus rainfall and a decreased amount of rainfall near the eastern part of the India is expected during the plus15 period. We may expect an intensification of the break period in the plus15 future period.

4.6.2 Active and break period of the *MIROC5* model for historical and plus20 period

Figure 26 shows the rainfall during the active and break period of the *MIROC5* model for the historical and plus20 period. Active period has slightly increased amount of rainfall over the core monsoon zone and decreased amount of rainfall over the eastern part of the India, in plus20 future period as compared to the historical period. During plus20 (future) breaks, there is an increased amount of rainfall near the foothills of the Himalayan region and less rainfall over the core monsoon zone.

4.7 Active and break period of the *NorESM1* model under 1.5°C and 2°C warming condition

4.7.1 Active and break period of the *NorESM1* model for historical and plus15 period

Figure 27 shows the rainfall during the active and break period of the *NorESM1* model for historical and plus15 period. A slightly increased amount of rainfall over the core monsoon zone, and near the eastern part of the India is expected during plus15 active. During plus15 (future) breaks, there is an increased amount of rainfall near the foothills of the Himalayan region, southern peninsula, and eastern part of the India and less rainfall over the core monsoon zone.

4.7.2 Active and break period of the *NorESM1* model for historical and plus20 period

Figure 28 shows the rainfall during the active and break period of the *NorESM1* model for historical and plus20 period. An increased amount of rainfall over the core monsoon zone is observed during the plus20 active period. During plus20 (future) breaks, there is an increased amount of rainfall near the foothills of

the Himalayan region, southern peninsula, and eastern part of the India and less rainfall over the core monsoon zone. It is important to note that although the rainfall during the breaks period will increase in northeast India, the rainfall over the core monsoon zone shows almost no sign of change as compared to the historical period

4.8 Active and break period of the ensemble mean of all model under 1.5°C and 2°C warming condition

4.8.1 Ensemble mean of all model for historical and plus15 period

Figure 29 shows the rainfall during the active and break period of ensemble mean of all models for historical and plus15 period. We have seen earlier with the individual model that in plus15 future period, there is slightly increased amount of rainfall over the core monsoon zone, ensemble mean of all model also shows similar kind of results i.e. intensification of the active period and increased amount of rainfall over the core monsoon zone and decreased amount of rainfall over the North-east part of the India. During plus15 (future) breaks, there is an increased amount of rainfall near the foothills of the Himalayan region, North-east part of the India, and less rainfall over the core monsoon zone. We may expect an intensification of the break period in plus15 future period. This condition certainly is not suitable for agricultural activities over the core monsoon zone and we may also expect increased agricultural drought during the future (plus15) period, which may adversely affect the agriculture sector of the country for which proper irrigation plans and policies may be planned towards the future.

4.8.2 Ensemble mean of all model for historical and plus20 period

Figure 30 shows the rainfall during the active and break period of ensemble mean of all models for historical and plus20 period. We have seen earlier with the individual model that in plus20 future period, there is a slightly increased amount of rainfall over the core monsoon zone, ensemble mean of all model also shows similar kind of results i.e. intensification of the active period and increased amount of rainfall over the core monsoon zone and decreased amount of rainfall over the North-east part of the India. During plus20 (future) breaks, there is an increased amount of rainfall over the North-east part of the India and less rainfall over the core monsoon zone. We may expect an intensification of the break period in plus20 future period. This condition is again not suitable for agricultural activities over the core monsoon zone and we may also expect increased agricultural drought during the future (plus20) period, which may adversely affect the agriculture sector of the country for which proper irrigation plans and policies may be planned towards the future.

4.9 VIMT (Vertically Integrated Moisture Transport) in the *NorESM1* model under 1.5°C and 2°C warming condition

4.9.1 Historical and plus15 period

Figure 31 shows the vertically integrated moisture transport in the *NorESM1* model for active and break period of historical and plus15 period. The active period during plus15 period shows an increase in moisture transport over the Arabian Sea and Bay of Bengal than during the historical period. There will be an intensification of the active period in plus15 future period and more rainfall over the core monsoon zone. During plus15 (future) breaks, there is an increased amount of moisture transport over the North-east part of the India, southern peninsula, near the foothills of the Himalayan region and less atmospheric moisture is being transported over the core monsoon zone.

4.9.2 Historical and plus20 period:

Figure 32 shows the vertically integrated moisture transport in the *NorESM1* model during active and break period of historical and plus20 period. The active period during plus20 period shows an increase in moisture transport over the Arabian Sea and Bay of Bengal than during the historical period. There will be an intensification of the active period in plus20 future period and more rainfall over the core monsoon zone. The break period during plus20 future period, shows a decrease in moisture transport over the Arabian Sea, as compared to the historical period. So there will be less rainfall over the core monsoon zone and more rainfall near the foothills of the Himalayan region and southern peninsula.

5.0 Summary And Conclusions

This section provides a summary of the research work and specific conclusions obtained from the results of the study. This also includes important findings and highlight a need for revisiting our water policy making for better water resources management.

5.1 Summary

Indian summer monsoon region is vulnerable to global warming which is evident in the form of an increasing number of extremes and the increasing spatial variability of rainfall. The main focus of the study is to understand the nature of the break and characteristics of the break over all India monsoon regions and how active and break will vary with warming? This study investigates the impacts of warming on the core monsoon zone and all India monsoon regions by using the output of the HAPPI experiment model. There are five AGCM models are used in this study such as *NorESM1-HAPPI*, *ECHAM6.3-LR*, *CanAM4*, *MIROC5*, and *CAM4-2degree*. These five AGCM models are part of the HAPPI experiment which provides climatic data such as precipitation for the historical period, plus15 period, and plus20 period. Since, only *NorESM1-HAPPI* model has precipitation, specific humidity, wind vector, and surface pressure data for the historical period, plus15 period and plus20 period as compared to the other four models used in this study, we selected *NorESM1-HAPPI* model for intra-model comparison (i.e. to identify the best run).

For further investigation of the intraseasonal variability, we considered all five AGCM models (i.e. inter-model comparison). The performance of each of these AGCMs in terms of historical climatology is tested with respect to the observed data (IMD) at a common grid ($1^\circ \times 1^\circ$) resolution. The active period and break period were identified using core monsoon zone rainfall for the historical and future period. Both inter-model and intra-model comparisons were performed based on indicators such as the frequency and length of active and break spells are for the historical period, plus15 period, and plus20 period (future).

The characteristics of active and break periods were compared in terms of frequency, magnitude, and spatial variability for the historical and future periods. Vertically integrated moisture transport is directly associated with the monsoon rainfall, therefore, VIMT pertaining to active and break were also analysed.

5.2 Conclusions

The key findings from the study are summarized as follows:

- Models such as *ECHAM6.3-LR*, *CAM4-2degree*, *MIROC5*, and *NorESM1-HAPPI* show significant change in the length of active period for historical, plus15, and plus20 period. We conclude that there is no significant increasing or decreasing trend in the length of active period for most of the models in the future except for the *NorESM1-HAPPI* model shows the significant increase in the length of active period for plus20 future. An increase in the length of the active period will results into more moisture during the plus20 future period than that of the historical period over the India and subcontinent region. There will be more rainfall over India and subcontinent region in future under 2°C warming condition.
- Models such as *CanAM4*, *CAM4-2degree*, and *NorESM1-HAPPI* show significantly change in the length of break period for historical, plus15, and plus20 period. We conclude that there is a significant increase in the length of the break period for all models in the future as compared to the historical period. An increase in the length of the break period in future will reduce moisture than that of the historical period over the India and subcontinent region in future. There will be relatively less rainfall over India and subcontinent region in future. So we can store a definite amount of water from the active period which will be used during the break period. Therefore, we will have to plan our irrigation system and agricultural activity accordingly towards a sustainable future period.
- Models such as *CanAM4*, *ECHAM6.3-LR*, *CAM4-2degree*, *MIROC5*, and *NorESM1-HAPPI* are significant for the frequency of active period for historical, plus15 and plus20 period. We conclude that there is a significant increase in the frequency of active period for most of the models in future except for the *ECHAM6.3-LR* model shows the significant decrease in the frequency of active period for plus15 future. An increase in the average number of active events and intensity is expected in the future active period. It will bring more frequent moisture in future periods than that of the historical period and there will be more intense rainfall in the future period.
- Models such as *CanAM4*, *ECHAM6.3-LR*, *CAM4-2degree*, *MIROC5*, and *NorESM1-HAPPI* show a significant change in frequency of break period for historical, plus15, and plus20 period. We conclude that there is a significant increase in the frequency of the break period for all models in

future as compared to the historical period. An increase in the average number of break events and intensity is observed towards the future period. It may be reduce moisture transport from the local oceanic sources during the future break period. There will be relatively less rainfall over India and subcontinent region in future due to the enhancement of breaks. It will create drought-like situations and adversely affect the agriculture sector of the country for which proper irrigation plans and policies may be planned towards the future.

- Results from different models such as *CanAM4*, *ECHAM6.3-LR*, *CAM4-2degree*, *MIROC5* and *NorESM1-HAPPI* shows that intensification of the active period in future under 1.5°C warming condition (plus15 future) and under 2°C warming condition (plus20 future) and there will be more rainfall over the core monsoon zone in the future period. Break period also shows an intensification of the break period in future under 1.5°C warming condition (plus15 future) and under 2°C warming condition (plus20 future) and there will be more rainfall near the foothills of the Himalayan region and southern peninsula.
- The vertically integrated moisture transport in *NorESM1* model, shows an increase in moisture transport in the future active period under 1.5°C warming condition (plus15 future) and under 2°C warming condition (plus20 future) and there will be more rainfall over the core monsoon zone and intensification of the active period. VIMT during break period shows a decrease in moisture transport and intensification of the break period in future under 1.5°C warming condition (plus15 future) and under 2°C warming condition (plus20 future) and there will be less rainfall over the core monsoon zone and more rainfall near the foothills of the Himalayan region and southern peninsula.

5.3 Way forward and scope of future research

The further scope of research is summarized below:

- For future assessment, it will be interesting to take seven best runs out of 120 runs of the *NorESM1* model for further investigation.
- Climatology of *MIROC5* Model is not good whereas climatology of *NorESM1-HAPPI* Model, *CanAM4 Model*, *CAM4-2degree* Model and *ECHAM6-3LR* Model are good. So for further analysis we can choose only these Models such as *NorESM1-HAPPI*, *CanAM4*, *CAM4-2degree* and *ECHAM6-3LR*.
- Investigation of the event to event rainfall variability for future period (2106-2115) under 1.5°C warming condition (plus15 future) and under 2°C warming condition (plus20 future). To capture the interconnectivity of adjacent wet and dry spells and the intensification of their phase shifts, event-to-event hydrological intensification index (E2E) combines normalized aggregated precipitation intensity (API) and dry spell length (DSL). Furthermore, it will be interesting to analyse these results in terms of the impact on other hydrological variables.

Declarations

Data availability

The high resolution HAPPI gridded ($1^{\circ}\times 1^{\circ}$) simulated datasets for period (2006-2015) current decade, Plus-15 (2106-2115) 1.5°C warming condition (future data) and Plus-20 (2106-2115) 2.0°C warming condition (future data) over entire India is freely available at

<https://portal.neresc.gov/c20c/data.html>

OR

https://portal.neresc.gov/cascade/data/downloader.php?get_dirs=

Code availability

The computations and some of the plots in this study area are prepared in MATLAB environment as well as in Linux Environment. These MATLAB and Linux codes are available from the corresponding author upon reasonable request.

Funding

This study is a part of the Master of Technology of research at IIT Kharagpur. There is no external funding. The author is very thankful to the Dr. Amey Pathak. The resources and facilities provided by the Agriculture and Food Engineering Department, IIT Kharagpur, are acknowledged.

Author information

Affiliations

Agriculture and Food Engineering Department, Indian Institute of Technology Kharagpur, West Bengal – 721302, India

Sumit Kumar Vishwakarma

Declaration of Interest Statement

The Indian Summer Monsoon Rainfall (ISMR) possesses a large amount of variability in terms of its spatial distribution and seasonal strength especially since post-industrialization period after the 1950s (Roxy 2018). Asian summer monsoon region is most vulnerable to global warming due to frequent occurrence of events such as heavy precipitation, heat waves, and drought (Lee et al., 2018).

Recently, it has been observed that the global mean sea-surface temperature is increasing and it due to rapid warming of the western tropical Indian Ocean (Roxy et al., 2014), (Roxy 2018). Furthermore, the western Indian Ocean went through a great extent of warming of 1.28°C in summer SSTs as compare to the Indian Ocean which experienced an increase of 0.78°C during 1901-2012 (Roxy 2018). Western Indian Ocean which is generally cool in nature as compared to the tropical warm Ocean alters the zonal SST gradients and has the ability to change the circulation characteristics and rainfall of the Asian monsoon (Roxy 2018). The propagation and initiation of the Monsoon Intraseasonal Oscillation (MISO) are mainly

governed by the ocean-atmospheric coupling of the Sea-Surface Temperature (SST), winds, convection and warming in the India ocean has an effect on its characteristics (Roxy 2018). The recent studies shows that as compared to the 1978-1988, northward-propagation characteristics of the MISO has changed during 2001-2011 due to the rapid increase in the SST temperature (Roxy 2018). Convection over the equatorial Indian Ocean is increased by the warming of the equatorial region which reduces the northward propagation of the MISO (Roxy 2018).

It is argued that, with respect to the pre-industrial period, an increase in 1.5°C global mean temperatures is projected to results in a 20% increase in daily rainfall, and under 2°C global mean temperature may results in a 25% increase in rainfall (Ali and Mishra, 2018).

At present, there is no study that focuses the impact of 1.5°C and 2°C warming on active and break spells in India, therefore, this study investigates the impacts of warming on the core monsoon zone and all India monsoon regions by using the output of the HAPPI experiment model. The purpose of this study is to provide detailed information of the future changes in active and break spells. The main focus of the study is to understand the nature of the break and characteristics of the break over all India monsoon regions under different target temperatures such as 1.5°C and 2°C and how active and break will vary with the warming?

References

1. Abhilash S, Sahai AK, Pattnaik S, De S (2013) Predictability during active break phases of Indian summer monsoon in an ensemble prediction system using climate forecast system. *J Atmos Solar Terr Phys* 100–101., 13–23. <https://doi.org/10.1016/j.jastp.2013.03.017>
2. Ali H, Mishra V (2018) Increase in Subdaily Precipitation Extremes in India Under 1.5 and 2.0°C Warming Worlds. *Geophys Res Lett* 45:6972–6982. <https://doi.org/10.1029/2018GL078689>
3. Annamalai H, Slingo JM (2001) Active/break cycles: Diagnosis of the intraseasonal variability of the Asian Summer Monsoon. *Clim Dyn* 18(1–2):85–102. doi:10.1007/s003820100161
4. Annamalai H, Sperber KR (2005) Regional heat sources and the active and break phases of boreal summer intraseasonal (30-50 day) variability. *J Atmos Sci* 62(8):2726–2748. doi:10.1175/JAS3504
5. Bhatla R, Ghosh S (2015) Study of break phase of Indian summer monsoon using different parameterization schemes of RegCM4. *3. Int J Earth Atmos Sci* 2(3):109–115
6. Blanford HF (1886) Rainfall of India. *Meteorology, India Meteorological Department* 2:217–448
7. Change C, Frontiers R (2007) Evaluation of the AR4 Climate Models ' Simulated Daily Maximum Temperature, Minimum Temperature, and Precipitation over Australia Using Probability 4356–4376. <https://doi.org/10.1175/JCLI4253.1>
8. De US, Mukhopadhyay RK (2002) Breaks in monsoon and related precursors. *Mausam* 53(3):309–318

9. Gadgil S (2003) The Indian monsoon and its variability. *Annu Rev Earth Planet Sci* 31(1):429–467. doi:10.1146/annurev.earth.31.100901.141251
10. Gadgil S, Joseph PV (2003) On breaks of the Indian monsoon. *Proceedings of the Indian Academy of Sciences, Earth and Planetary Sciences*, 112(4), 529–558. doi:10.1007/BF02709778
11. Gimeno L, Vázquez M, Eiras-Barca J, Sorí R, Stojanovic M, Algarra I, Nieto R, Ramos AM, Durán-Quesada AM, Dominguez F (2020) Recent progress on the sources of continental precipitation as revealed by moisture transport analysis. *Earth Sci Rev* 201:103070. <https://doi.org/10.1016/j.earscirev.2019.103070>
12. Goswami BN, Wu G, Yasunari T (2006) The annual cycle, intraseasonal oscillations, and roadblock to seasonal predictability of the Asian summer monsoon. *J Clim* 19(20):5078–5099. doi:10.1175/JCLI3901
13. Goswami BN, Xavier PK (2003) Potential predictability and extended range prediction of Indian summer monsoon breaks. *Geophys Res Lett* 30(18):1–4. <https://doi.org/10.1029/2003GL017810>
14. Krishnamurthy V, Shukla J (2008) Seasonal persistence and propagation of intraseasonal patterns over the Indian monsoon region. *Clim Dyn* 30(4):353–369. doi:10.1007/s00382-007-0300-7
15. Krishnan R, Zhang C, Sugi M (2000) Dynamics of breaks in the Indian summer monsoon. *J Atmos Sci* 57(9):1354–1372. doi:10.1175/1520-0469
16. Lakshmi DD, Satyanarayana ANV, Chakraborty A (2019) Assessment of heavy precipitation events associated with floods due to strong moisture transport during summer monsoon over India. *J Atmos Solar Terr Phys* 189:123–140. <https://doi.org/10.1016/j.jastp.2019.04.013>
17. Lee D, Min S, Fischer E, Shiogama H, Bethke I (2018) Impacts of half a degree additional warming on the Asian summer monsoon rainfall characteristics. *Environmental research letters* 13:044033
18. Li Z, Sun Y, Li T, Ding Y, Hu T (2019) Future Changes in East Asian Summer Monsoon Circulation and Precipitation Under 1.5 to 5°C of Warming. *Earth's Future* 7:1391–1406. <https://doi.org/10.1029/2019EF001276>
19. Lisa VAlexanderX, Zhang HJ, Fowler C, Tebaldi A, Lynch NT, Issue TS, Union AG, Iugg T (2009) Climate extremes: progress and future directions. *Int J Climatol* 29(3):317–319. <https://doi.org/10.1002/joc>
20. Madakumbura GD, Kim H, Utsumi N, Shiogama H, Fischer EM, Seland, Mitchell DM (2019) Event-to-event intensification of the hydrologic cycle from 1.5°C to a 2.0°C warmer world. *Sci Rep* 9(1):3483. doi:10.1038/s41598-019-39936-2
21. Ma Y, Lu M, Chen H, Pan M, Hong Y (2018) Atmospheric moisture transport versus precipitation across the Tibetan Plateau: A mini-review and current challenges. *Atmos Res* 209:50–58. <https://doi.org/10.1016/j.atmosres.2018.03.015>
22. Mitchell D, Achutarao K, Allen M, Bethke I, Beyerle U, Ciavarella A, Forster PM, Fuglestedt J, Gillett N, Haustein K, Ingram W, Iversen T (2017) Half a degree additional warming, prognosis and projected impacts (HAPPI): background and experimental design. *Geosci Model Dev* 571–583. <https://doi.org/10.5194/gmd-10-571-2017>

23. Mohan RA, Goswami BN (2000) A common spatial mode for intra-seasonal and inter-annual variation and predictability of the Indian summer monsoon. *Current Science*, 1106–1111
24. Muraleedharan PM, Mohankumar K, Sivakumar KU (2013) A study on the characteristics of temperature inversions in active and break phases of Indian summer monsoon. *J Atmos Solar Terr Phys* 93:11–20. doi:10.1016/j.jastp.2012.11.006
25. Narayana Rao T, Saikranthi K, Radhakrishna B, Vijaya Bhaskara Rao S (2016) Differences in the climatological characteristics of precipitation between active and break spells of the Indian summer monsoon. *J Clim* 29(21):7797–7814. doi:10.1175/jcli-d-16-0028.1
26. Ordóñez P, Ribera P, Gallego D, Peña-ortiz C (2012) Major moisture sources for Western and Southern India and their role on synoptic-scale rainfall events. *Hydrol Process* 3895:3886–3895. <https://doi.org/10.1002/hyp.8455>
27. Pai DS, Sridhar L, Kumar R, M.R (2016) Active and break events of Indian summer monsoon during 1901–2014. *Clim Dyn* 46:3921–3939. <https://doi.org/10.1007/s00382-015-2813-9>
28. Pathak A, Ghosh S, Kumar P (2014) Precipitation recycling in the Indian subcontinent during summer monsoon. *J Hydrometeorol* 15:2050–2066. <https://doi.org/10.1175/JHM-D-13-0172.1>
29. Pathak A, Ghosh S, Alejandro Martinez J, Dominguez F, Kumar P (2017) Role of oceanic and land moisture sources and transport in the seasonal and interannual variability of summer monsoon in India. *J Clim* 30:1839–1859. <https://doi.org/10.1175/JCLI-D-16-0156.1>
30. Pillai PA, Sahai AK (2014) Moist dynamics of active/break cycle of Indian summer monsoon rainfall from NCEPR2 and MERRA reanalysis. *Int J Climatol* 34(5):1429–1444. <https://doi.org/10.1002/joc.3774>
31. Polanski S, Fallah B, Befort DJ, Prasad S, Cubasch U (2014) Regional moisture change over India during the past Millennium: A comparison of multi-proxy reconstructions and climate model simulations. *Glob Planet Change* 122:176–185. <https://doi.org/10.1016/j.gloplacha.2014.08.016>
32. Prasad VS, Hayashi T (2007) Active, weak and break spells in the Indian summer monsoon. *Meteorological and Atmospheric Physics* 95:53–61. <https://doi.org/10.1007/s00703-006-0197-4>
33. Raghavan K (1973) Break-Monsoon Over India. *Mon Weather Rev* 101(1):33–43. doi:10.1175/1520-0493
34. Rai SK, Kumar S, Rai AK, Palsaniya DR (2014) Climate Change, Variability and Rainfall Probability for Crop Planning in Few Districts of Central India. *Atmospheric and Climate Sciences* 04(03):394–403. <https://doi.org/10.4236/acs.2014.43039>
35. Rajeevan M, Bhate J, Kale JD, Lal B (2006) High resolution daily gridded rainfall data for the Indian region: Analysis of break and active monsoon spells. *Curr Sci* 91(3):296–306
36. Rajeevan M, Gadgil S, Bhate J (2010) Active and break spells of the indian summer monsoon. *J Earth Syst Sci* 119:229–247. <https://doi.org/10.1007/s12040-010-0019-4>
37. Ramesh Kumar MR, Prabhu Dessai UR (2004) A new criterion for identifying breaks in monsoon conditions over the Indian subcontinent. *Geophys Res Lett* 31(18):6–8. doi:10.1029/2004gl020562

38. Roxy, M. K., Ritika, K., Terray, P., & Masson, S. (2014). The curious case of Indian Ocean warming. *Journal of Climate*, 27(22), 8501–8509. doi:10.1175/jcli-d-14-00471.
39. Roxy Mathew Koll, C. S. T. (2018). Impacts of Climate Change on the Indian Summer Monsoon Chapter. *Climate Change and Water Resources in India*, 21–37. doi:10.1080/02626667.2012.702213.
40. Shrivastava S, Kar SC, Sharma AR (2017) Intraseasonal Variability of Summer Monsoon Rainfall and Droughts over Central India. *Pure appl Geophys* 174(4):1827–1844. doi:10.1007/s00024-017-1498
41. Sikka DR, Gadgil S (1980) On the maximum cloud zone and the ITCZ over Indian longitudes during the southwest monsoon. *Mon Weather Rev* 108(11):1840–1853. doi:10.1175/1520-0493
42. Singh C (2013) Characteristics of monsoon breaks and intraseasonal oscillations over central India during the last half century. *Atmos Res* 128:120–128. doi:10.1016/j.atmosres.2013.03.003
43. Singh D, Tsiang M, Rajaratnam B, Diffenbaugh NS (2014) Observed changes in extreme wet and dry spells during the south Asian summer monsoon season. *Nature Climate Change* 4(6):456–461. doi:10.1038/nclimate2208
44. Sudeepkumar BL, Babu CA, Varikoden H (2018) Future projections of active-break spells of Indian summer monsoon in a climate change perspective. *Glob Planet Change* 161:222–230. doi:10.1016/j.gloplacha.2017.12.020
45. Sinha N, Chakraborty S, Chattopadhyay R, Goswami BN, Mohan PM, Parua DK, Sarma D, Datye A, Sengupta S, Bera S, Baruah KK (2019) Isotopic investigation of the moisture transport processes over the Bay of Bengal. *Journal of Hydrology X* 2:100021. <https://doi.org/10.1016/j.hydroa.2019.100021>
46. Sudeepkumar BL, Babu CA, Varikoden H (2018) Future projections of active-break spells of Indian summer monsoon in a climate change perspective. *Glob Planet Change* 161:222–230. <https://doi.org/10.1016/j.gloplacha.2017.12.020>
47. Suhas E, Neena JM, Goswami BN (2012) Interannual variability of indian summer monsoon arising from interactions between seasonal mean and intraseasonal oscillations. *J Atmos Sci* 69:1761–1774. <https://doi.org/10.1175/JAS-D-11-0211.1>
48. Uhe PF, Mitchell DM, Bates PD, Sampson CC, Smith AM, Islam AS (2019) Enhanced flood risk with 1.5 °c global warming in the Ganges-Brahmaputra-Meghna basin. *Environmental Research Letters* 14(7). doi:10.1088/1748-9326/ab10ee
49. Ullah K, Gao S (2012) Moisture transport over the Arabian Sea associated with summer rainfall over Pakistan in 1994 and 2002. *Adv Atmos Sci* 29:501–508. <https://doi.org/10.1007/s00376-011-0200-y>
50. Umakanth U, Kesarkar AP, Rao TN, Rao SVB (2015) An objective criterion for the identification of breaks in Indian summer monsoon rainfall. *Atmospheric Science Letters* 16(3):193–198. doi:10.1002/asl2.536
51. Wang B, Webster PJ, Teng H (2005) Antecedents and self-induction of active-break south Asian monsoon unraveled by satellites. *Geophys Res Lett* 32(4):1–4. <https://doi.org/10.1029/2004GL020996>

52. Webster PJ, Holland GJ, Curry JA, Chang HR (2005) Atmospheric science: Changes in tropical cyclone number, duration, and intensity in a warming environment. *Science* 309(5742):1844–1846. <https://doi.org/10.1126/science.11164>
53. Webster PJ, Magaña VO, Palmer TN, Shukla J, Tomas RA, Yanai M, Yasunari T (1998) Monsoons: Processes, predictability, and the prospects for prediction. *Journal of Geophysical Research: Oceans* 103(7):14451–14510. doi:10.1029/97jc02719
54. Woo S (2018) Projected changes in summer precipitation over East Asia with a high-resolution atmospheric general circulation model during 21st century. *Environment Research Letters* 4610–4631. <https://doi.org/10.1002/joc.5727>
55. Yetbarek E, Ojha R (2020) Spatio-temporal variability of soil moisture in a cropped agricultural plot within the Ganga Basin, India. *Agric Water Manage* 234:106108. <https://doi.org/10.1016/j.agwat.2020.10610>
56. Zhang W, Zhou T, Zou L, Zhang L, Chen X (2018) Reduced exposure to extreme precipitation from 0.5°C less warming in global land monsoon regions. *Nat Commun* 1–8., 2041–1723. <https://doi.org/10.1038/s41467-018-05633-3>
57. Woo, S. (2018). Projected changes in summer precipitation over East Asia with a high-resolution atmospheric general circulation model during 21st century. *Environment Research Letters*, 4610–4631. <https://doi.org/10.1002/joc.5727>
58. Yetbarek, E., Ojha, R., (2020). Spatio-temporal variability of soil moisture in a cropped agricultural plot within the Ganga Basin, India. *Agricultural Water Management*, 234, 106108. <https://doi.org/10.1016/j.agwat.2020.10610>
59. Zhang, W., Zhou, T., Zou, L., Zhang, L., & Chen, X. (2018). Reduced exposure to extreme precipitation from 0.5°C less warming in global land monsoon regions. *Nature Communications*, 1–8, 2041-1723. <https://doi.org/10.1038/s41467-018-05633-3>

Figures

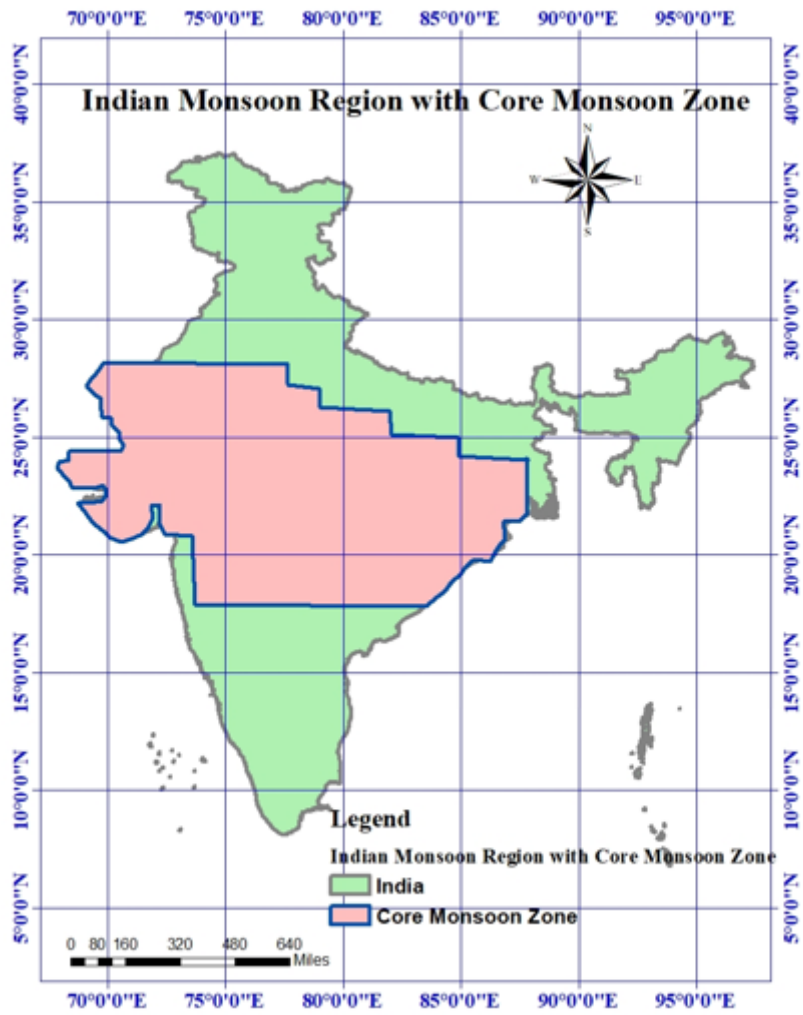


Figure 1

Map of the study area

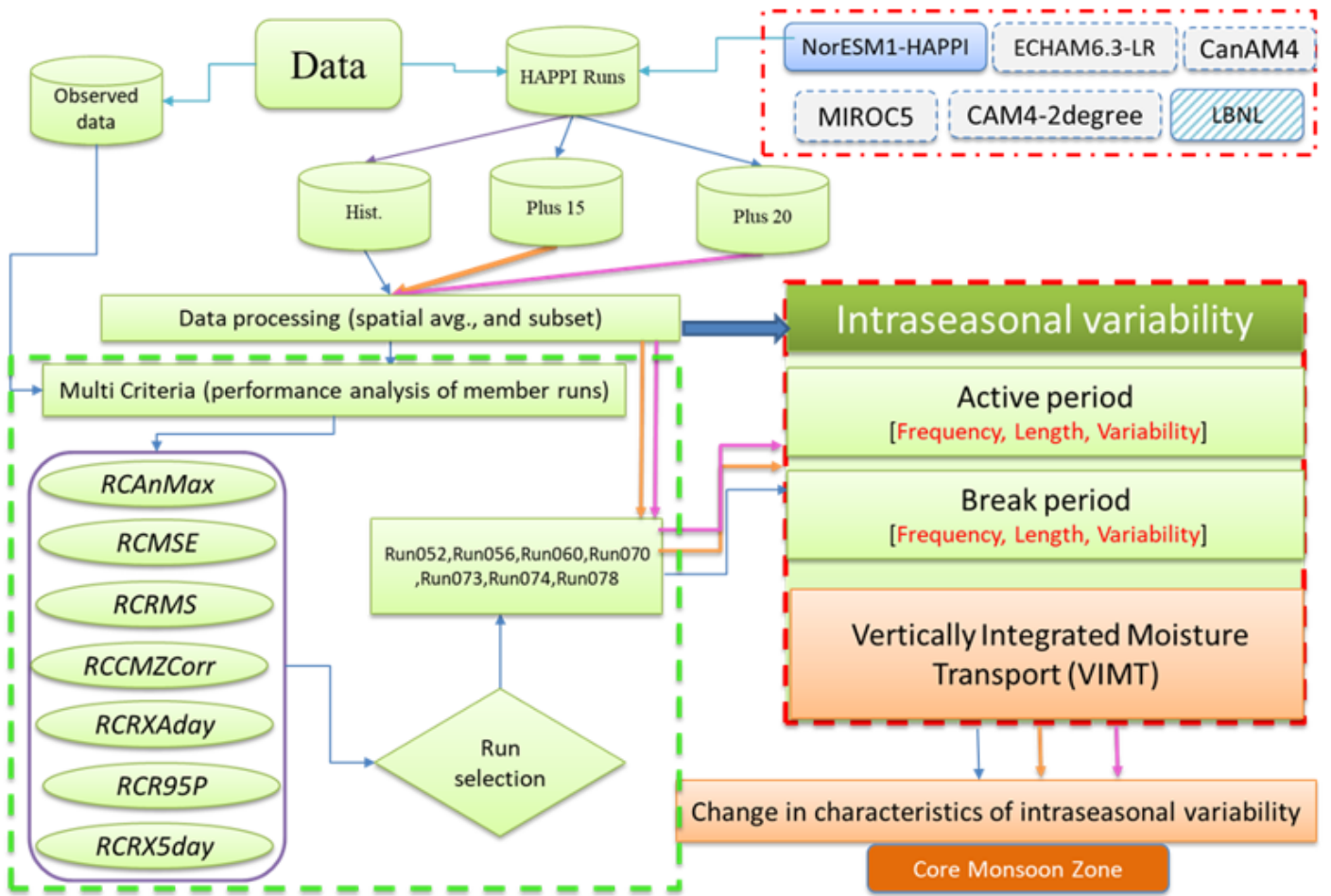


Figure 2

Flowchart summarizing of the workflow.

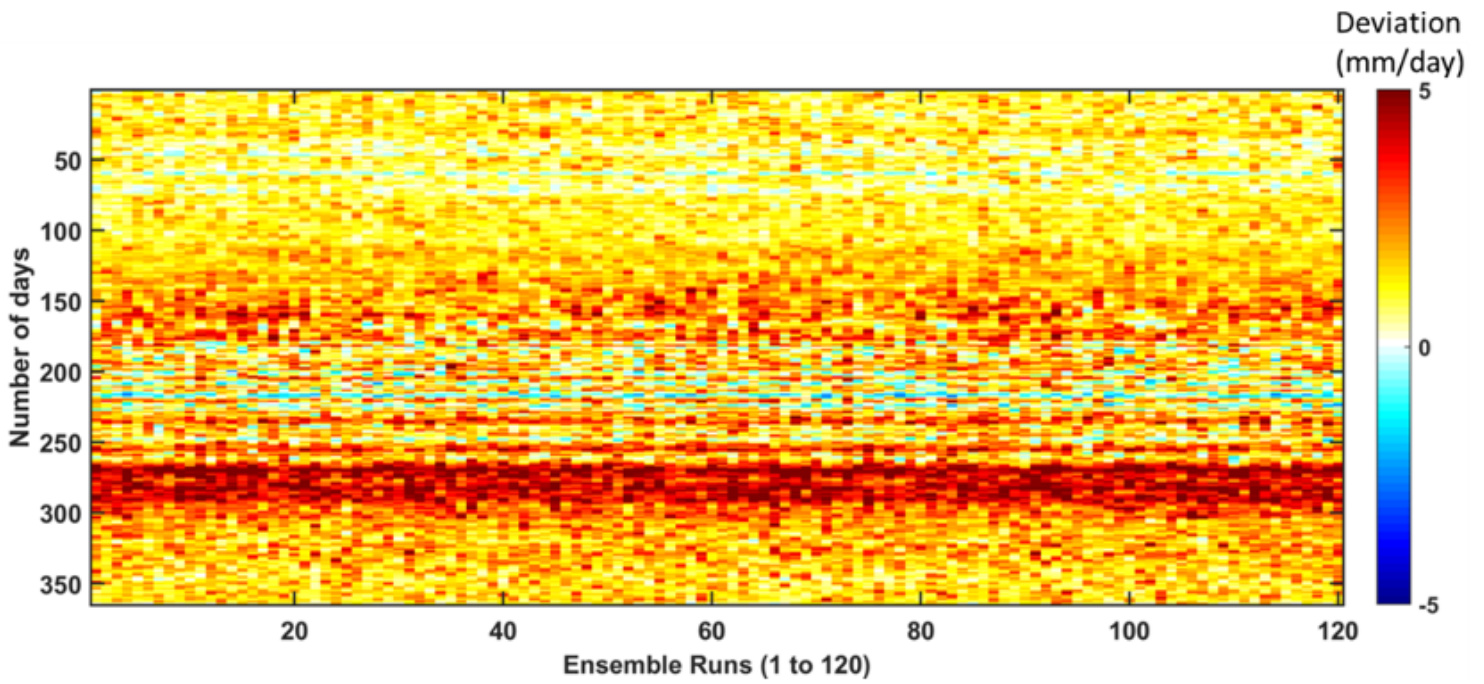


Figure 3

Deviation of long term AIMR climatology from the observed data (IMD).

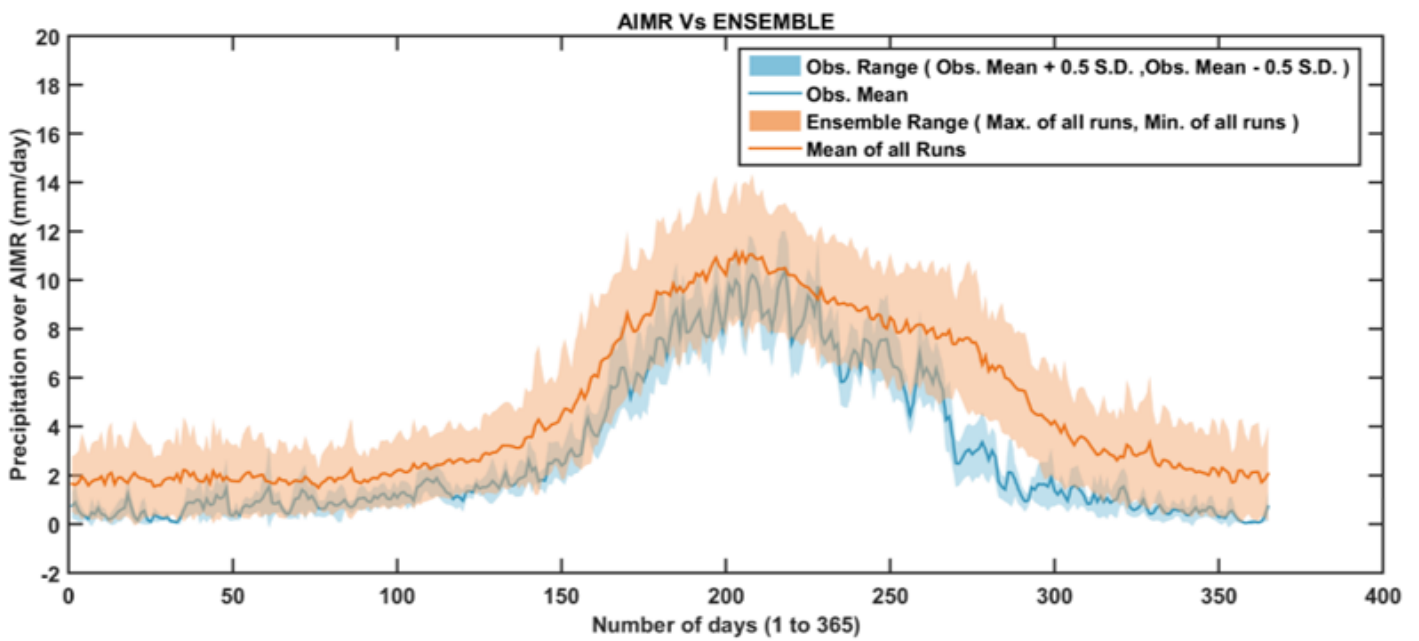


Figure 4

Comparison between different ensembles run with respect to IMD in terms of long term daily climatology.

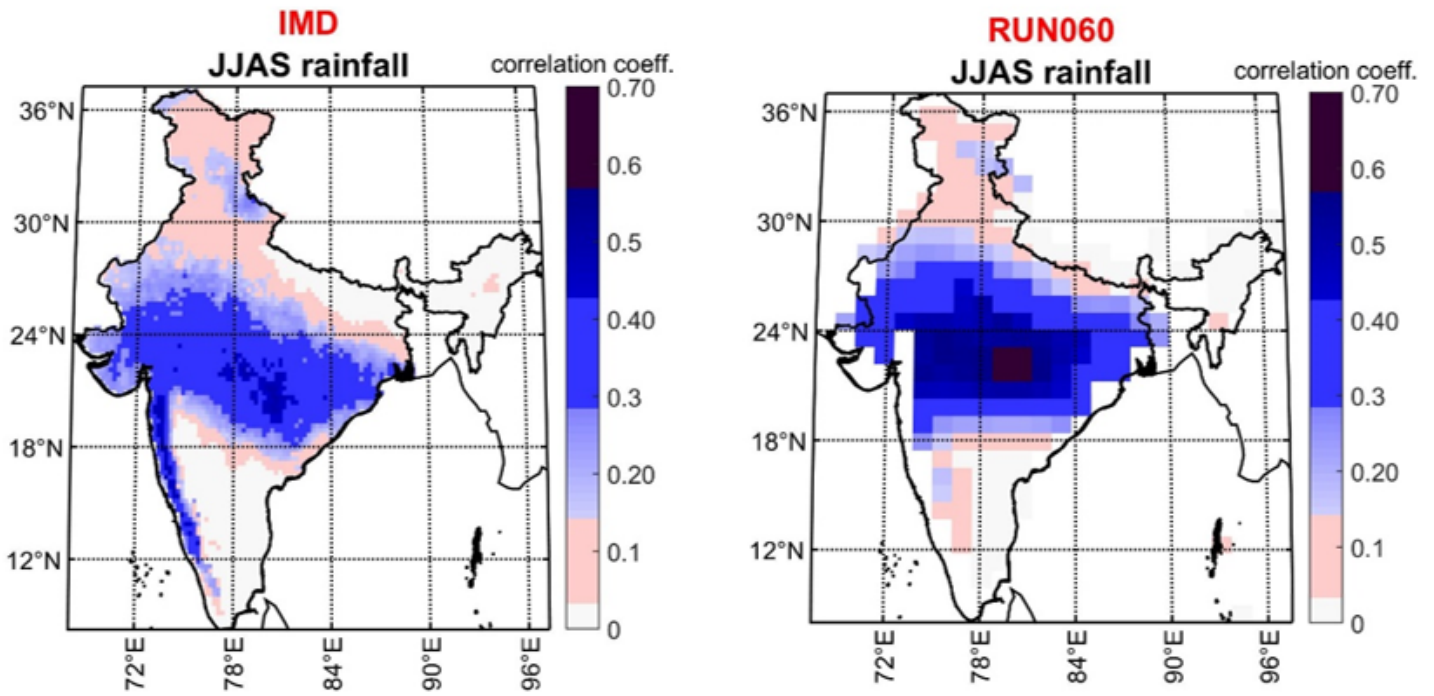


Figure 5

Correlation between CMZ and rainfall over all India nodes (a) IMD, and (b) run060.

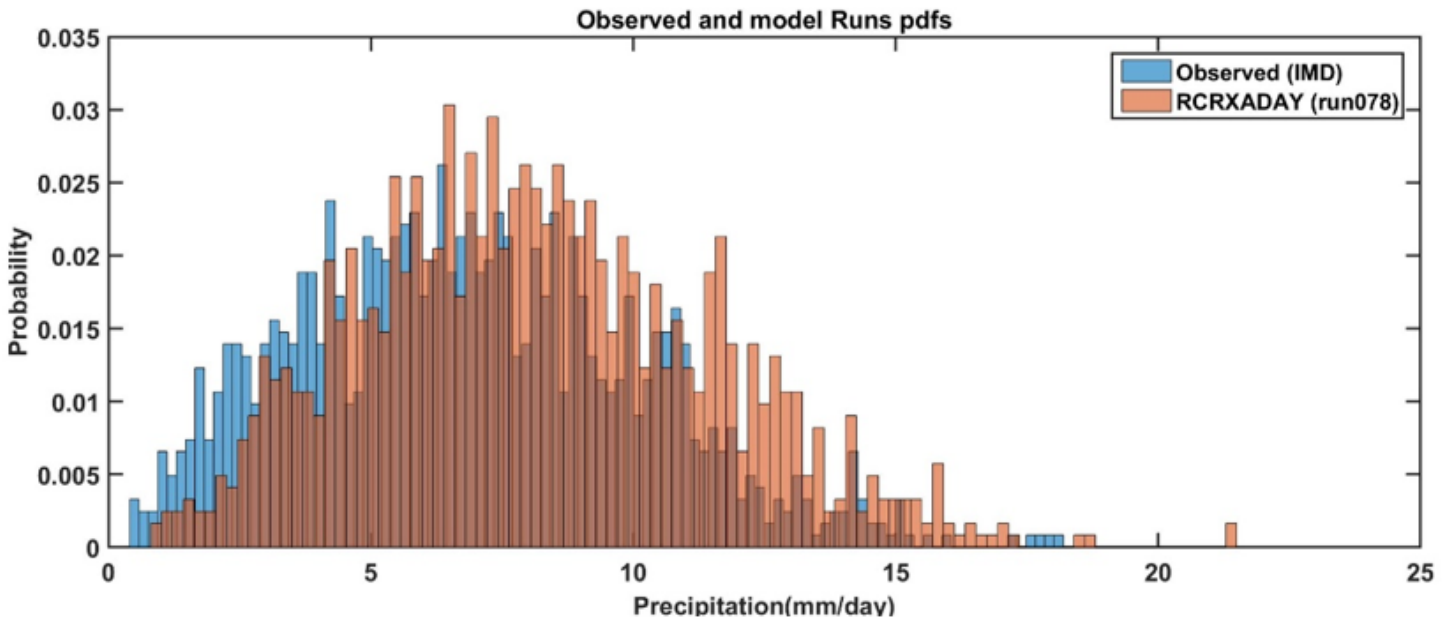


Figure 6

Comparison of skill score between observed data and run078.

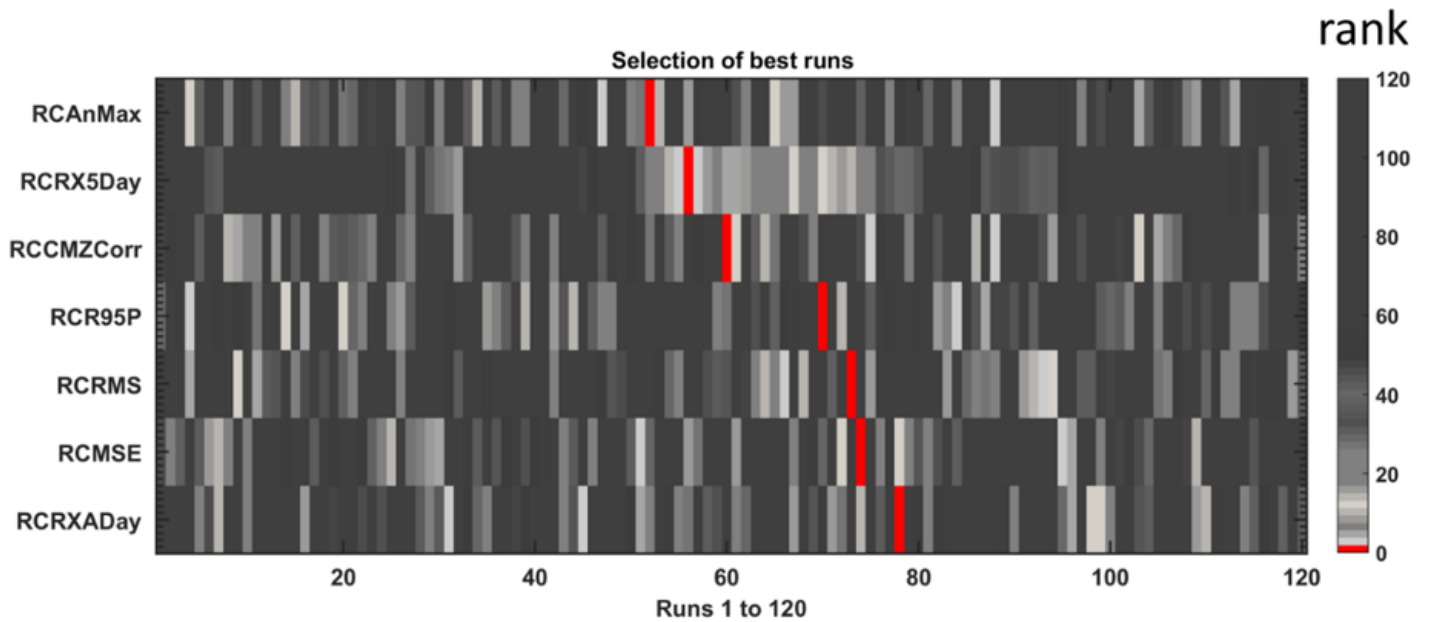


Figure 7

Selection of best runs based on different criteria.

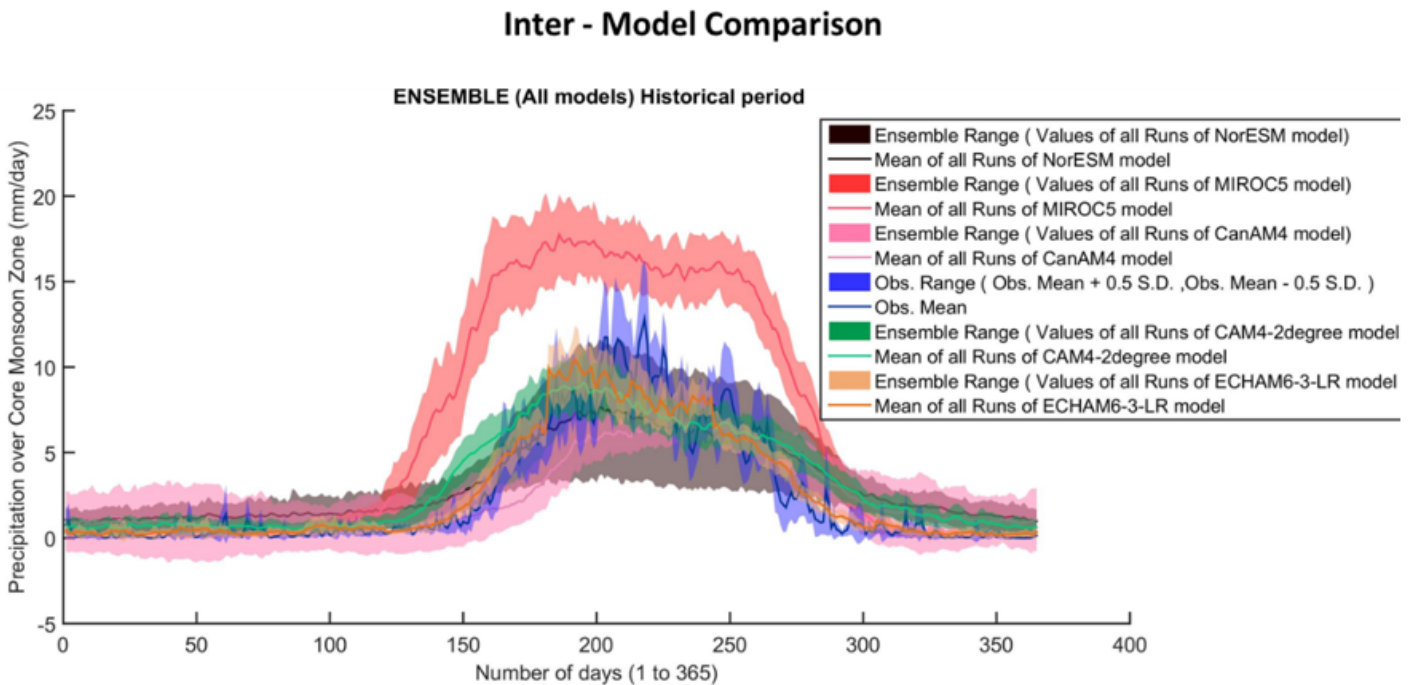


Figure 8

Comparison of climatology of five AGCM models w.r.t. IMD during historical period.

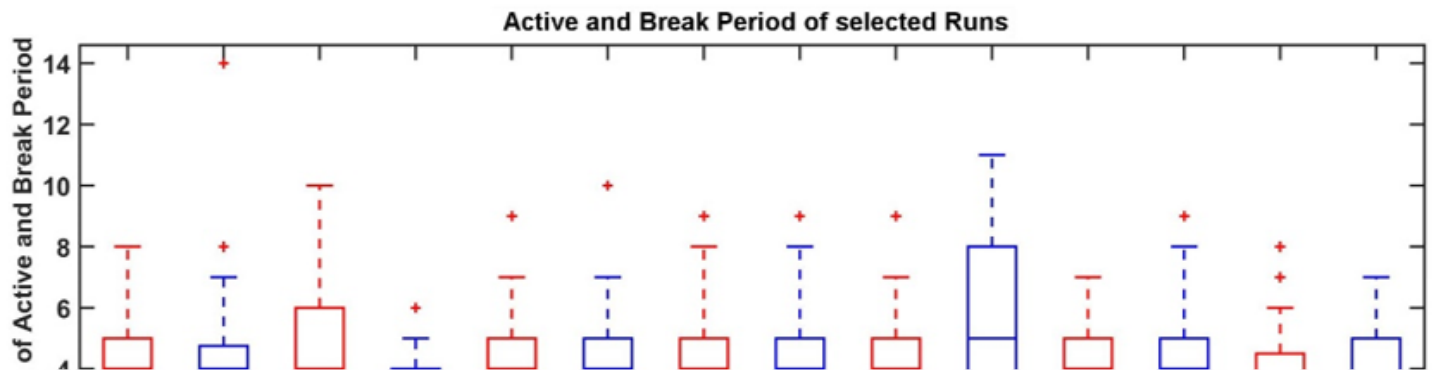


Figure 9

Length of active and break period of selected runs for the *NorESM1-HAPPI* model.

Image not available with this version

Figure 10

This image is not available with this version.

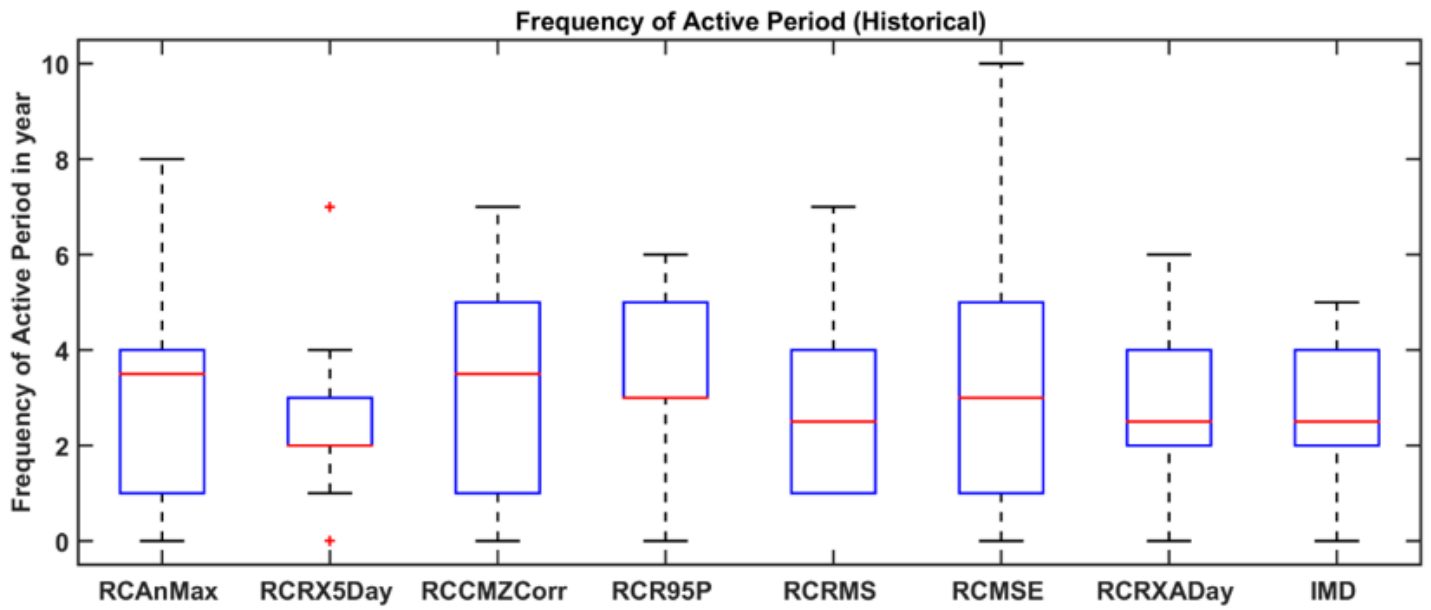


Figure 11

Frequency of active period for selected runs of the *NorESM1-HAPPI* model.

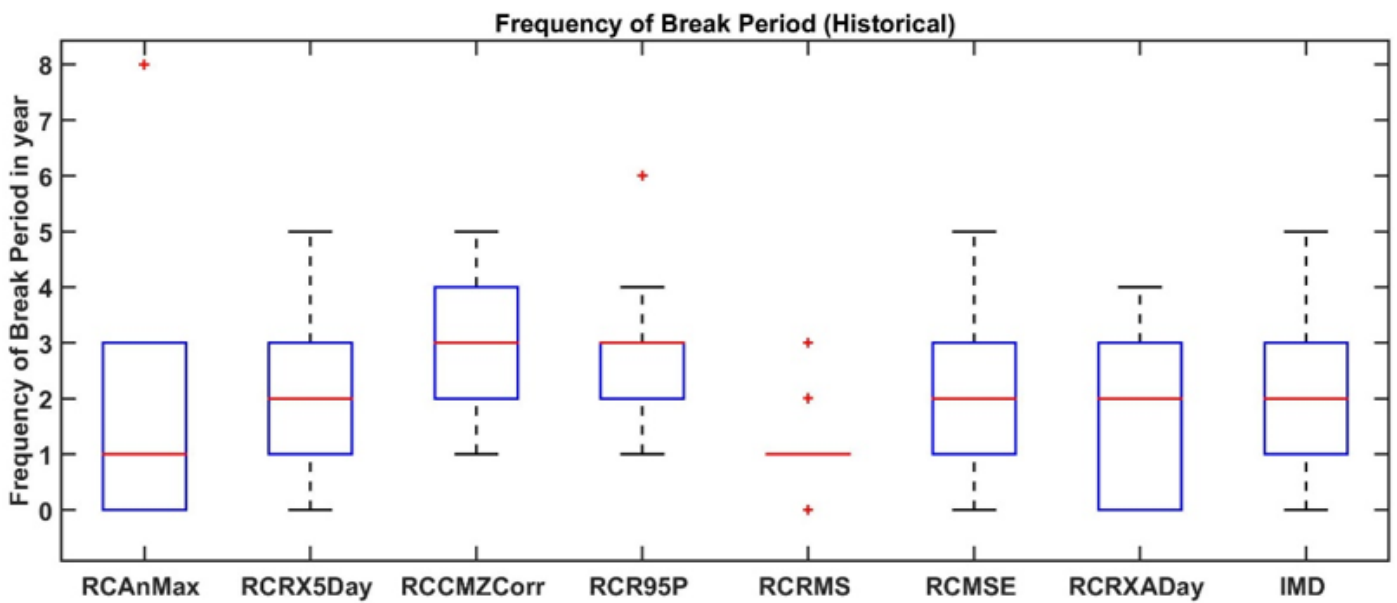


Figure 12

Frequency of break period of selected runs for the *NorESM1-HAPPI* model.

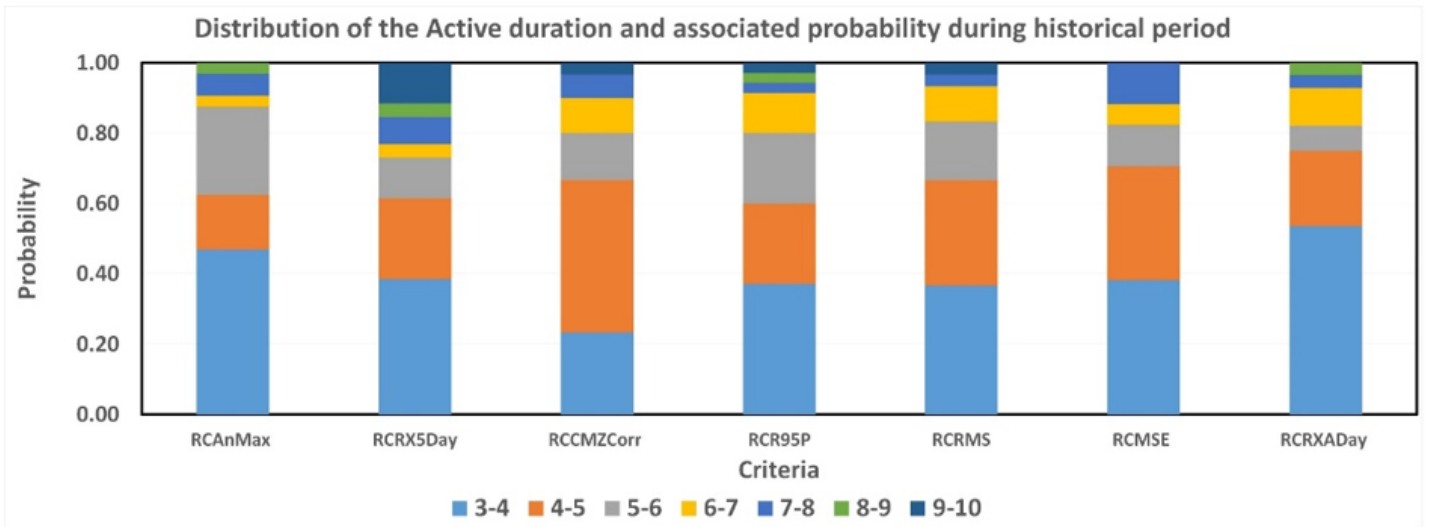


Figure 13

Distribution of the active duration and associated probability during the historical period for the *NorESM1-HAPPI* model. [Note: Here, colour represents the number of days]

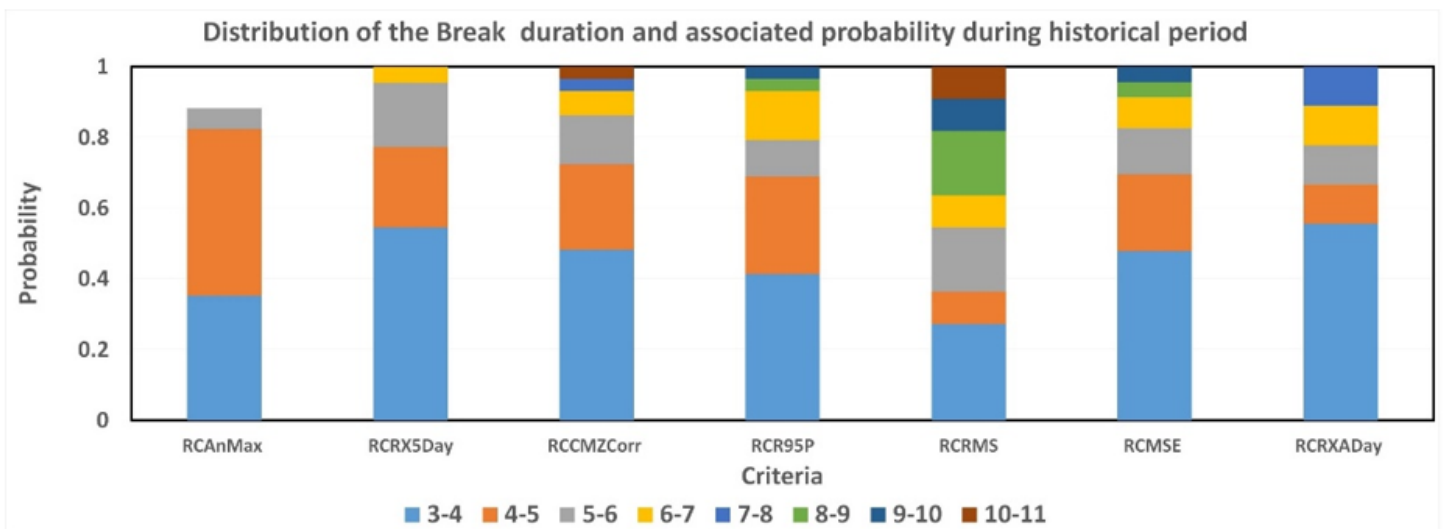


Figure 14

Distribution of the break duration and associated probability during the historical period for the *NorESM1-HAPPI* model. [Note: Here, colour represents the number of days]

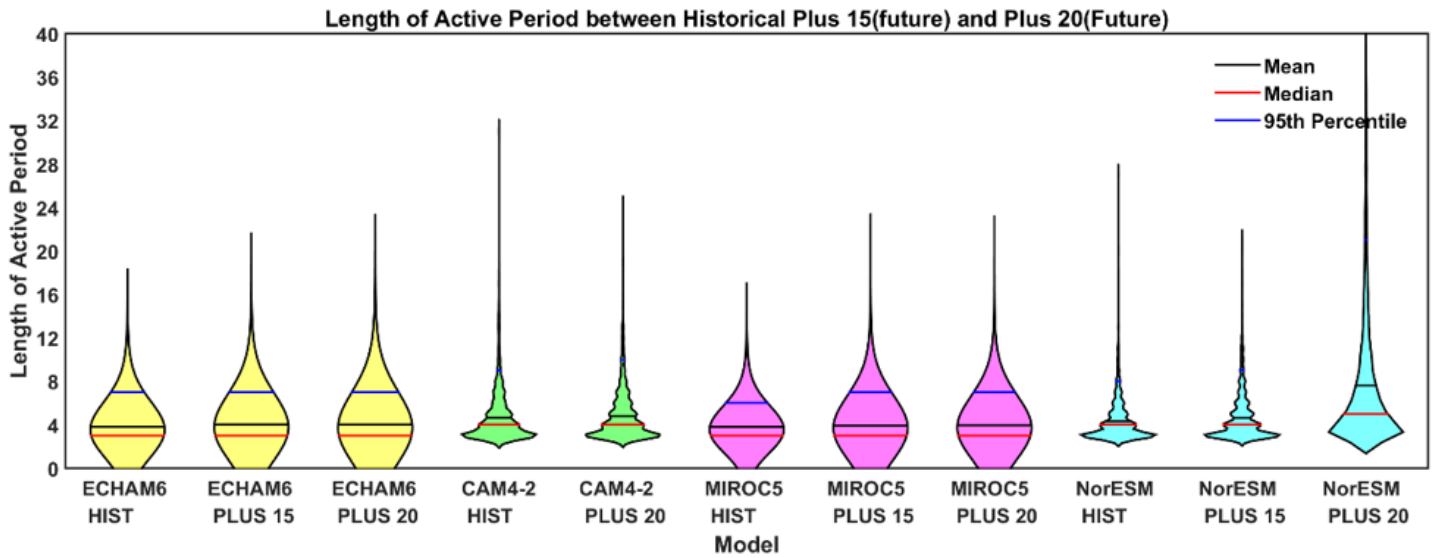


Figure 15

Length of the active period between historical, plus15 (future), and plus20 (future).

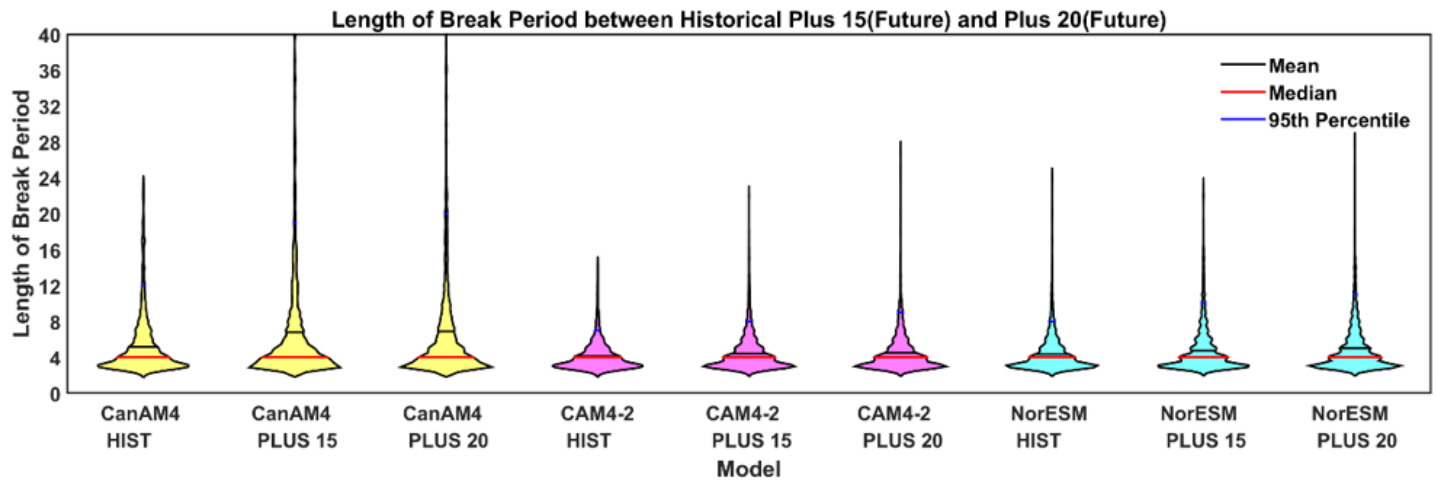


Figure 16

Length of break period between historical, plus15 (future), and plus20 (future).

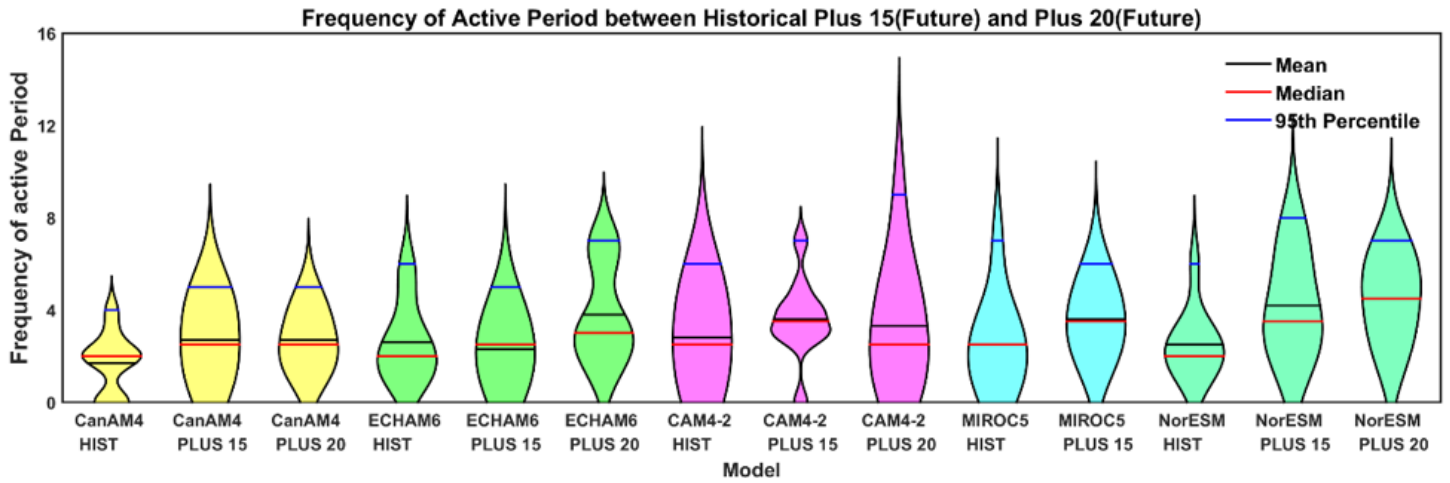


Figure 17

Frequency of active period between historical, plus15 (future), and plus20 (future).

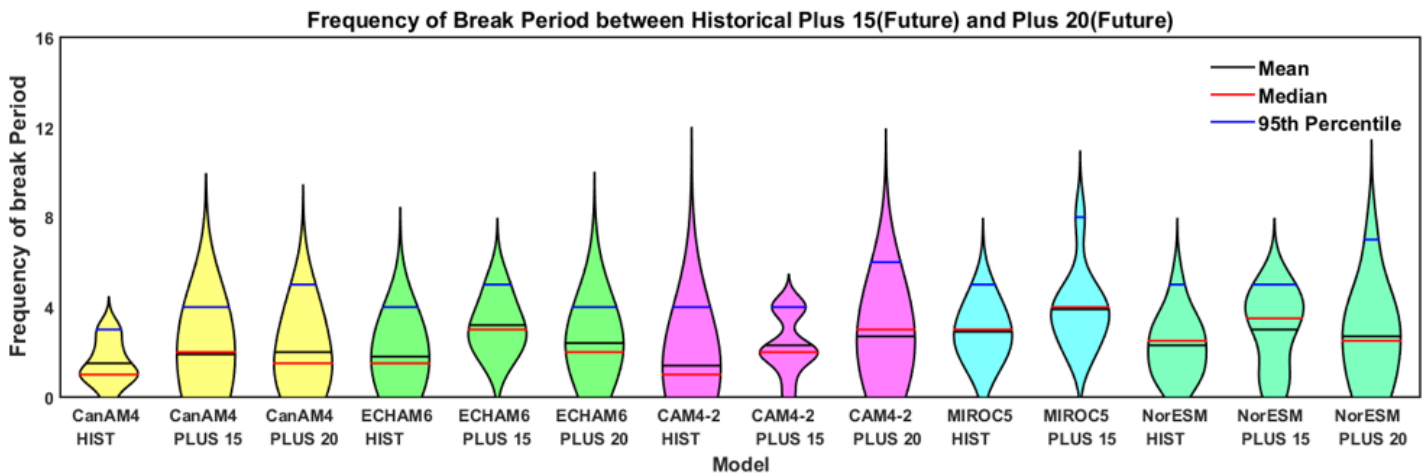


Figure 18

Frequency of break period between historical, plus15 (future), and plus20 (future).

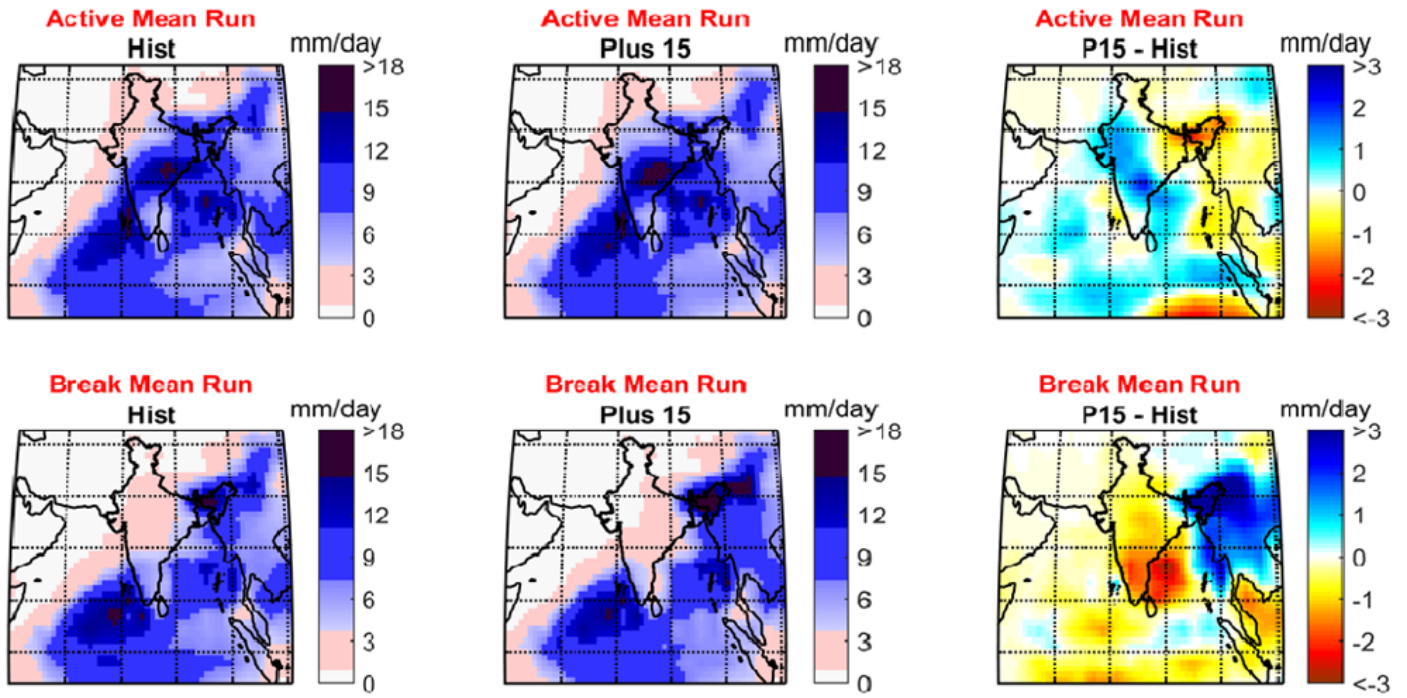


Figure 19

Active and break period rainfall in the *CanAM4* model for historical and plus15 future period (1.5°C warming condition).

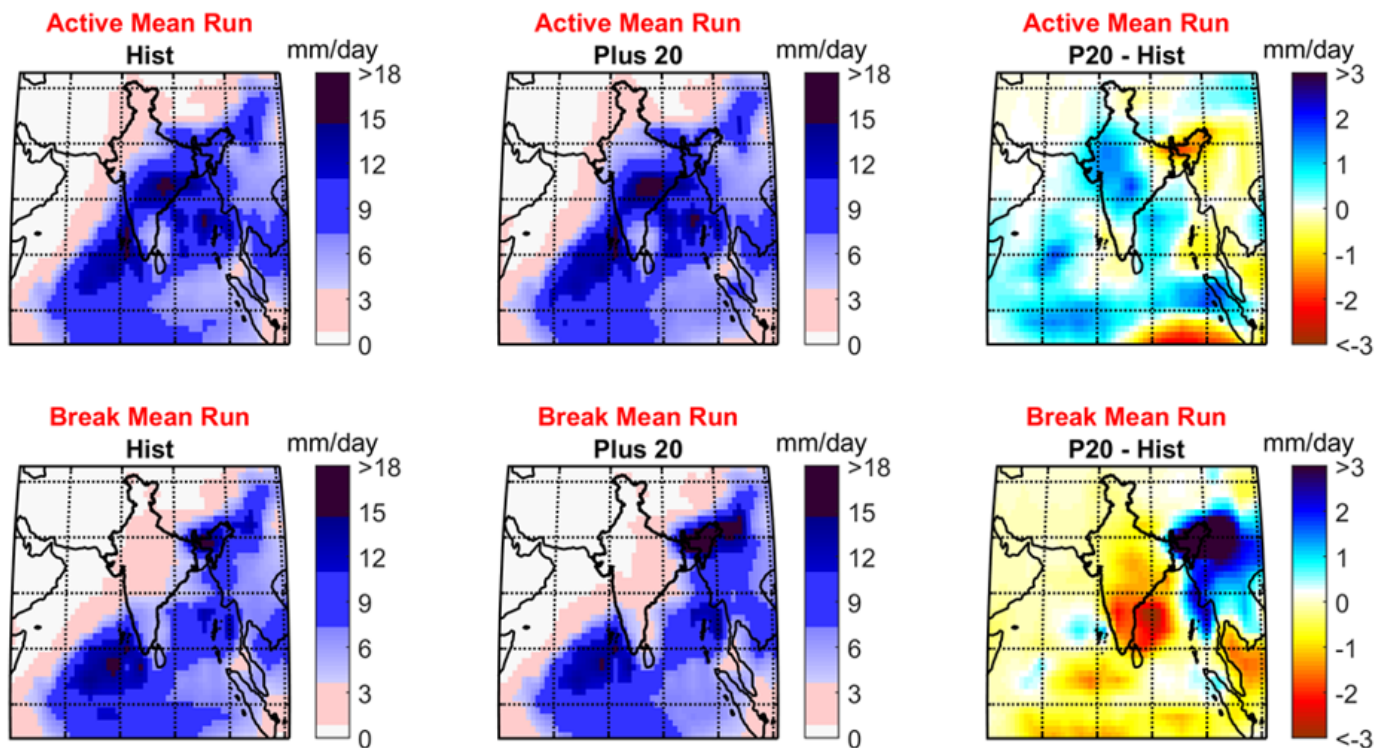


Figure 20

Active and break period rainfall in the *CanAM4* model for historical and plus20 future period (2°C warming condition).

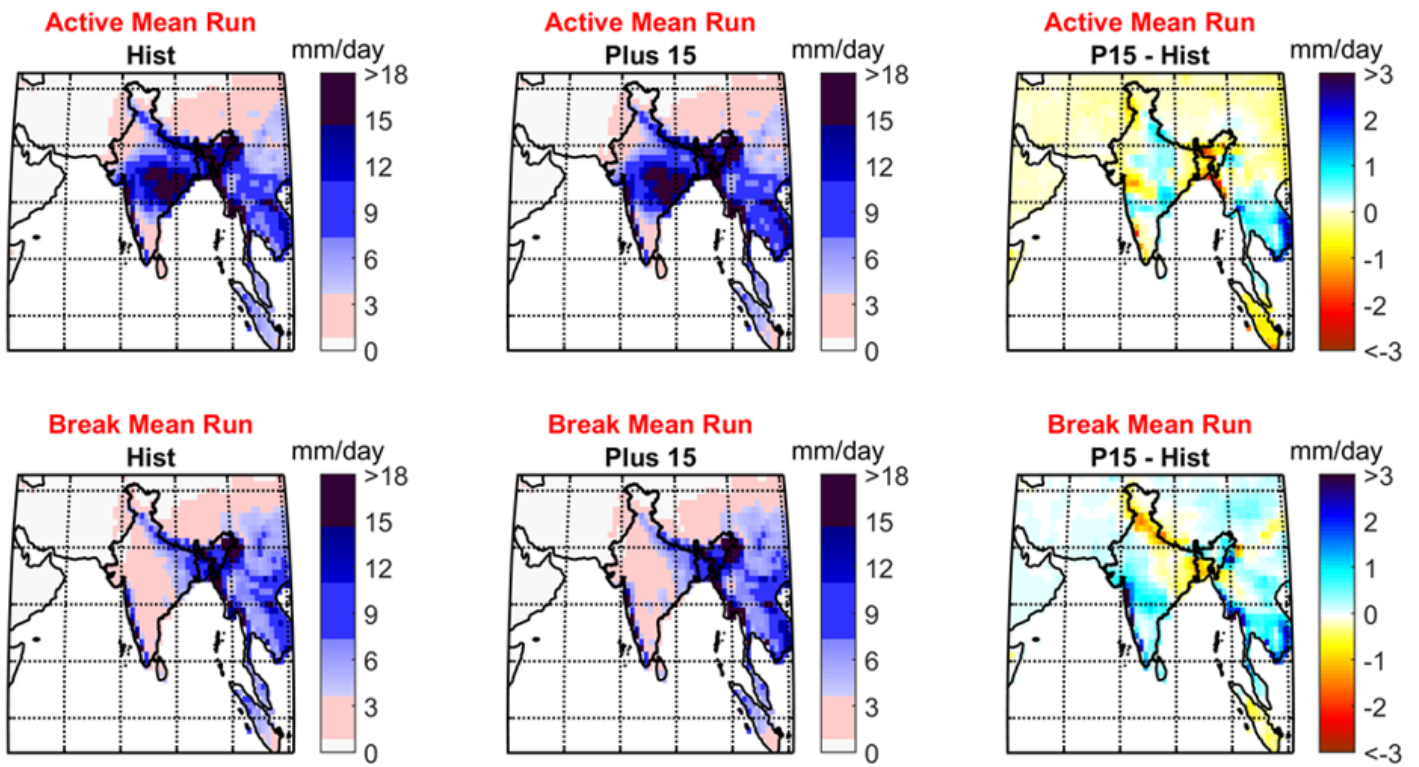


Figure 21

Active and break period rainfall in the *ECHAM6-3LR* model for historical and plus15 future period (1.5°C warming condition).

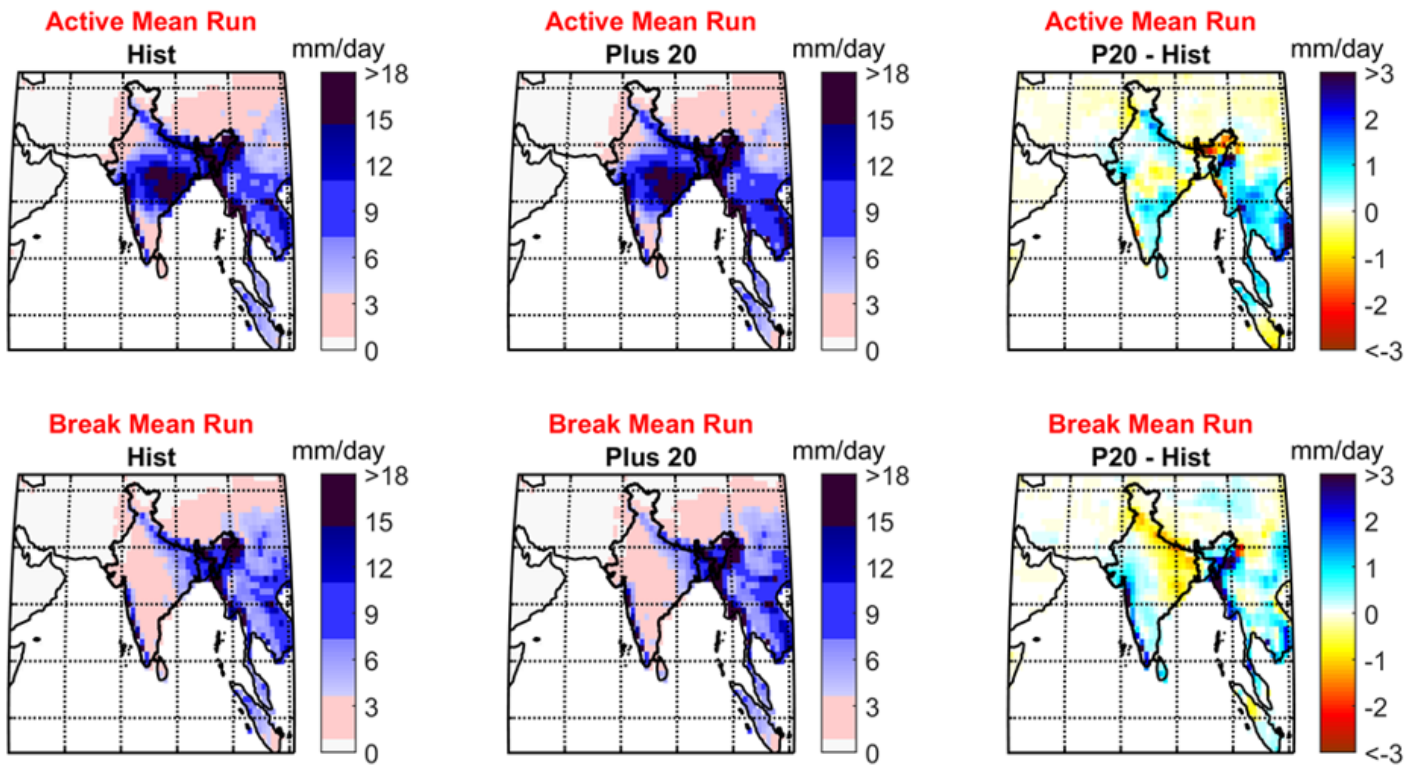


Figure 22

Active and break period rainfall in the *ECHAM6-3LR* model for historical and plus20 future period (2°C warming condition).

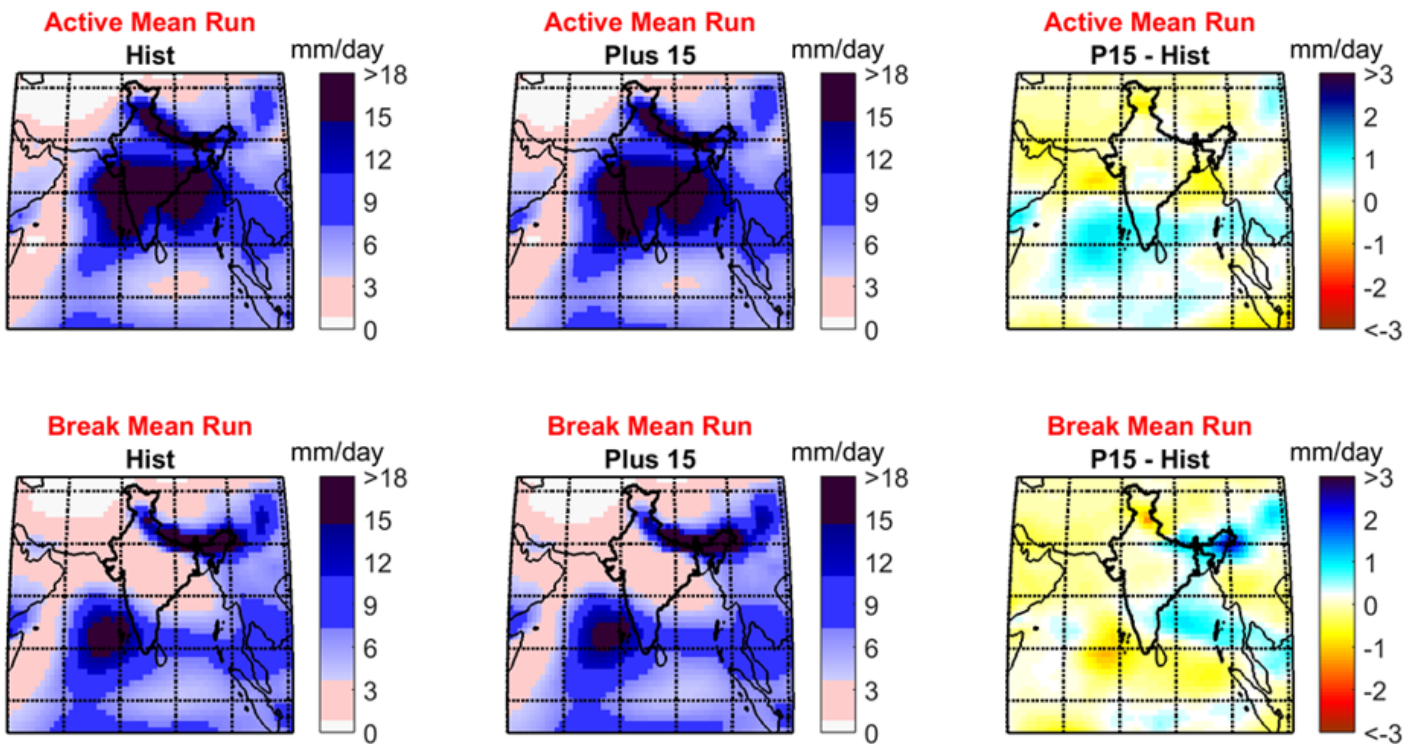


Figure 23

Active and break period rainfall in the *CAM4-2degree* model for historical and plus15 future period (1.5°C warming condition).

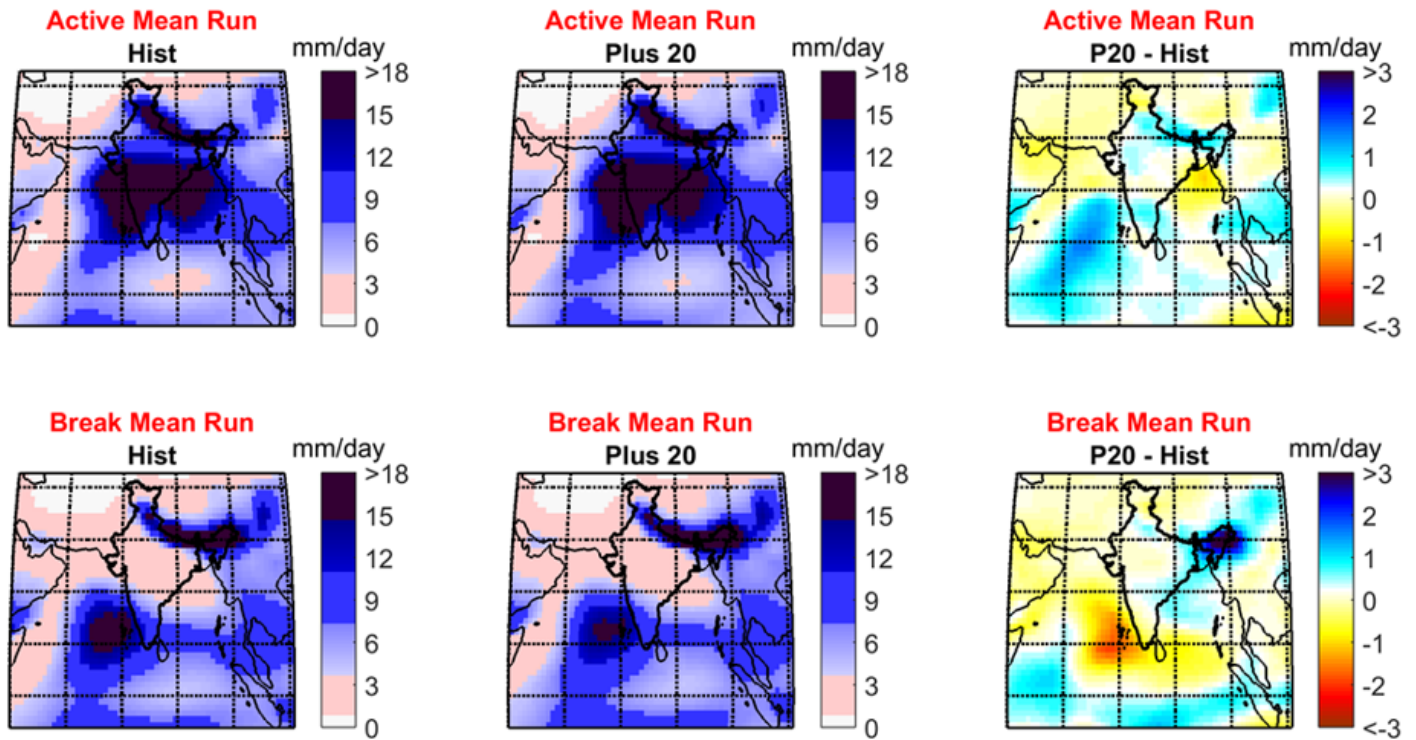


Figure 24

Active and break period rainfall in the *CAM4-2degree* model for historical and plus20 future period (2°C warming condition).

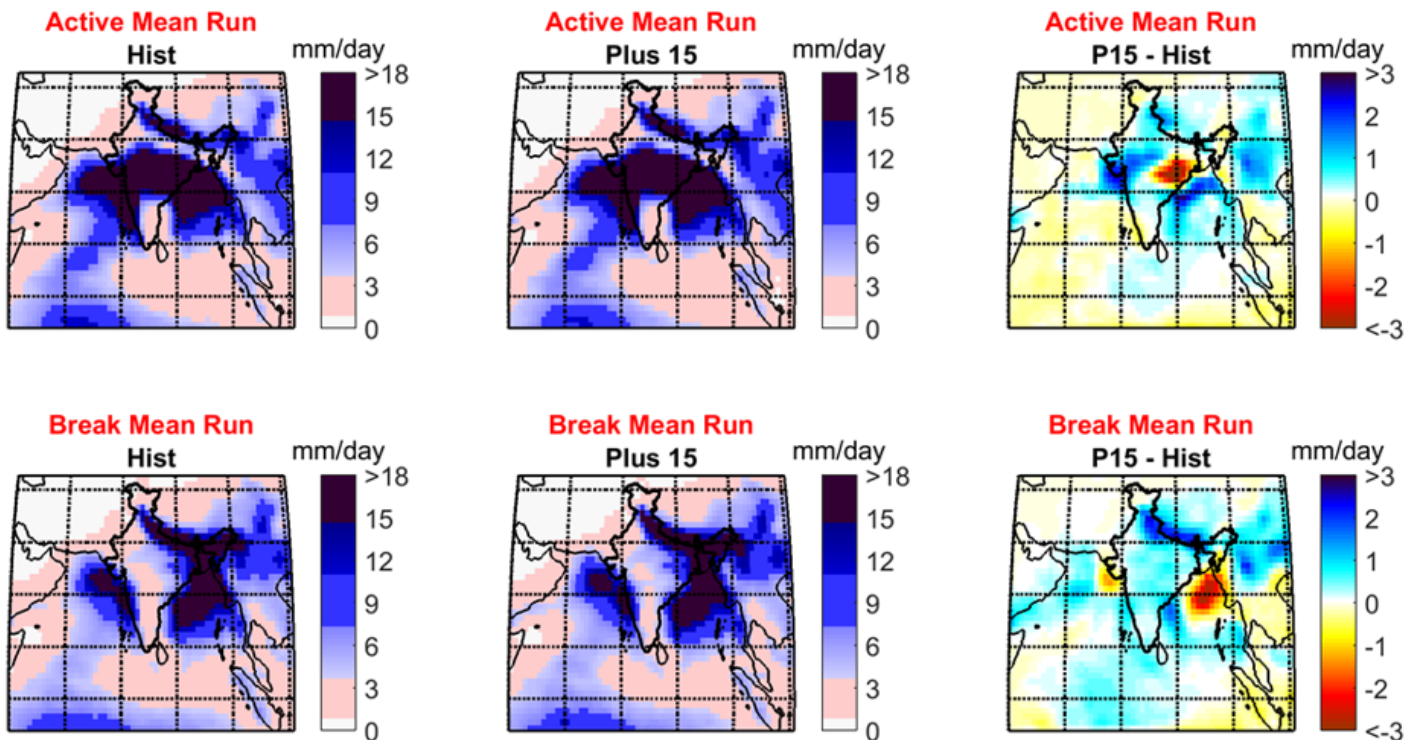


Figure 25

Active and break period rainfall in the *MIROC5* model for historical and plus15 future period (1.5°C warming condition).

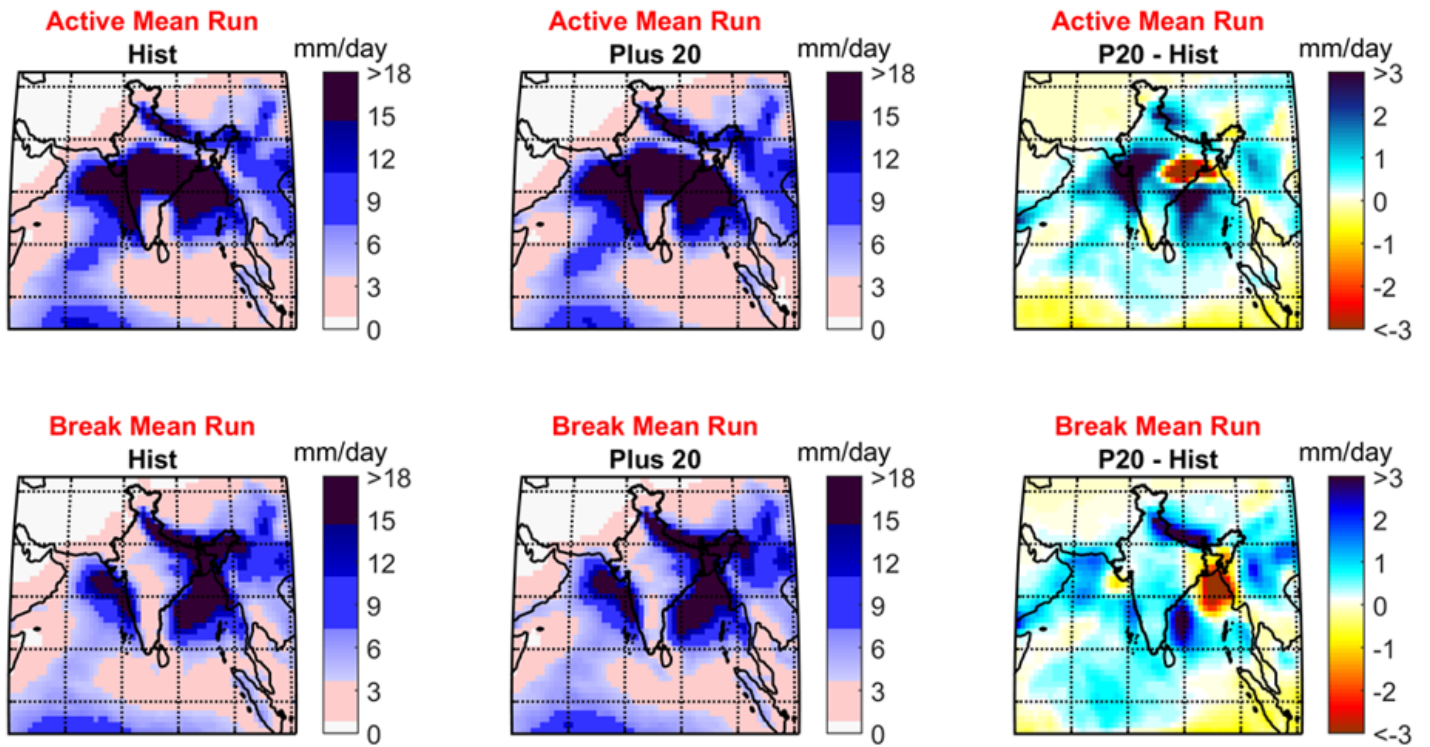


Figure 26

Active and break period rainfall in the *MIROC5* model for historical and plus20 future period (2°C warming condition).

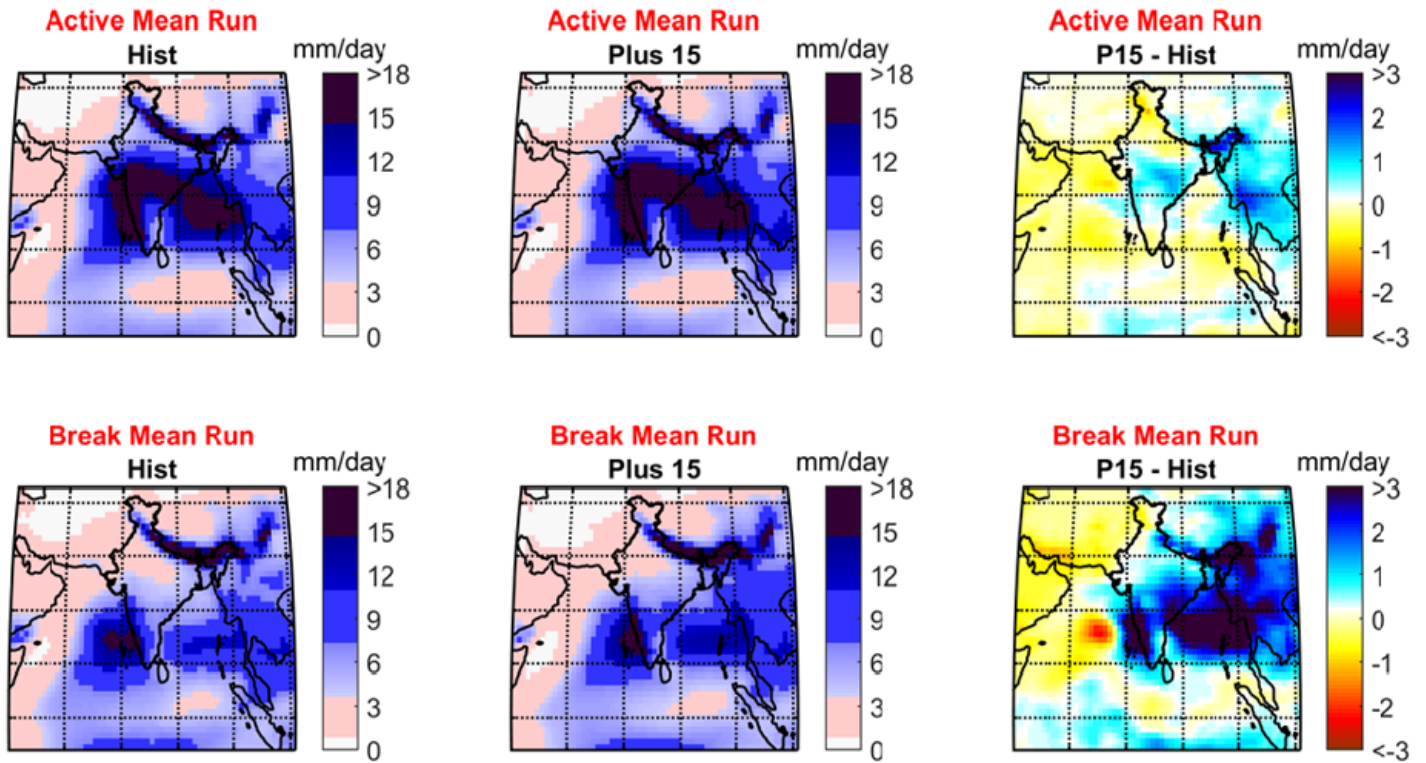


Figure 27

Active and break period rainfall in the *NorESM1* model for historical and plus15 future period (1.5°C warming condition).

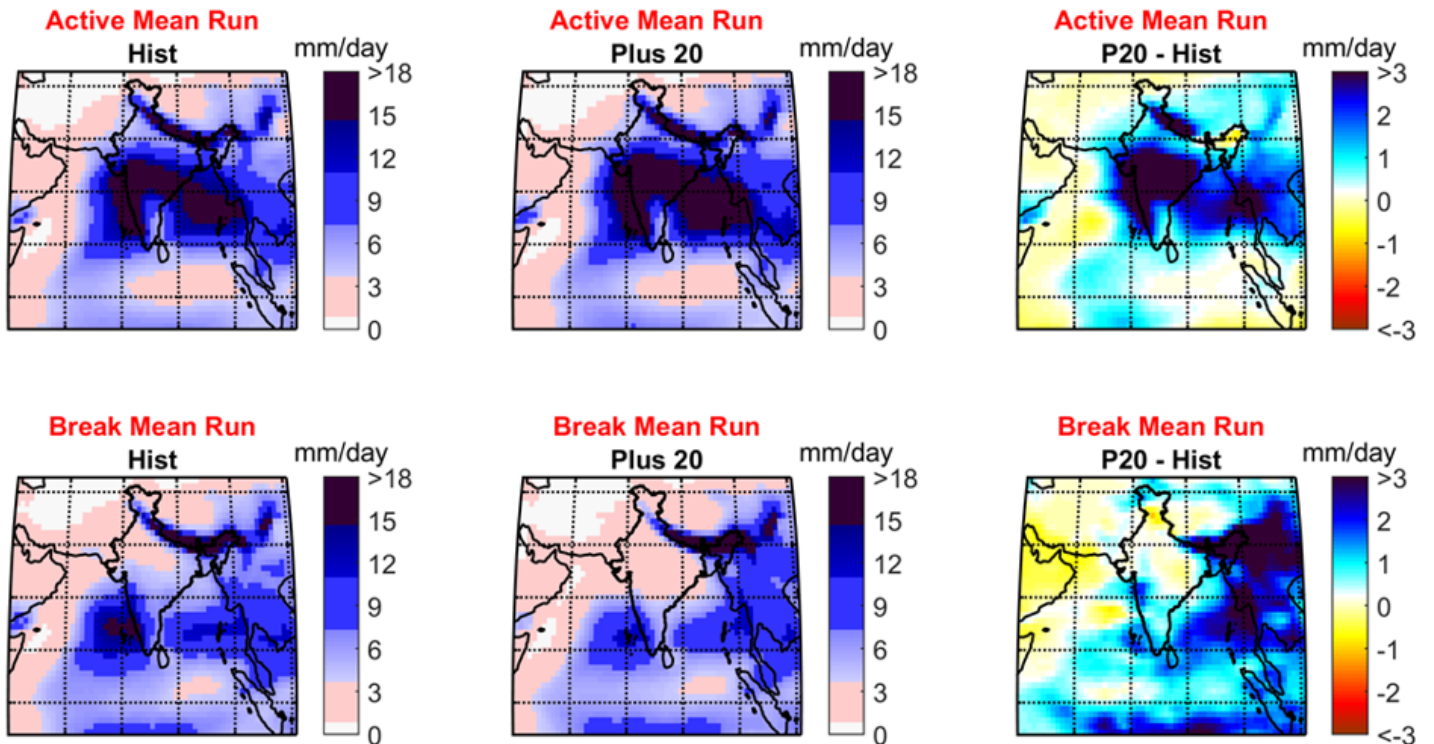


Figure 28

Active and break period rainfall in the *NorESM1* model for historical and plus20 future period (2°C warming condition).

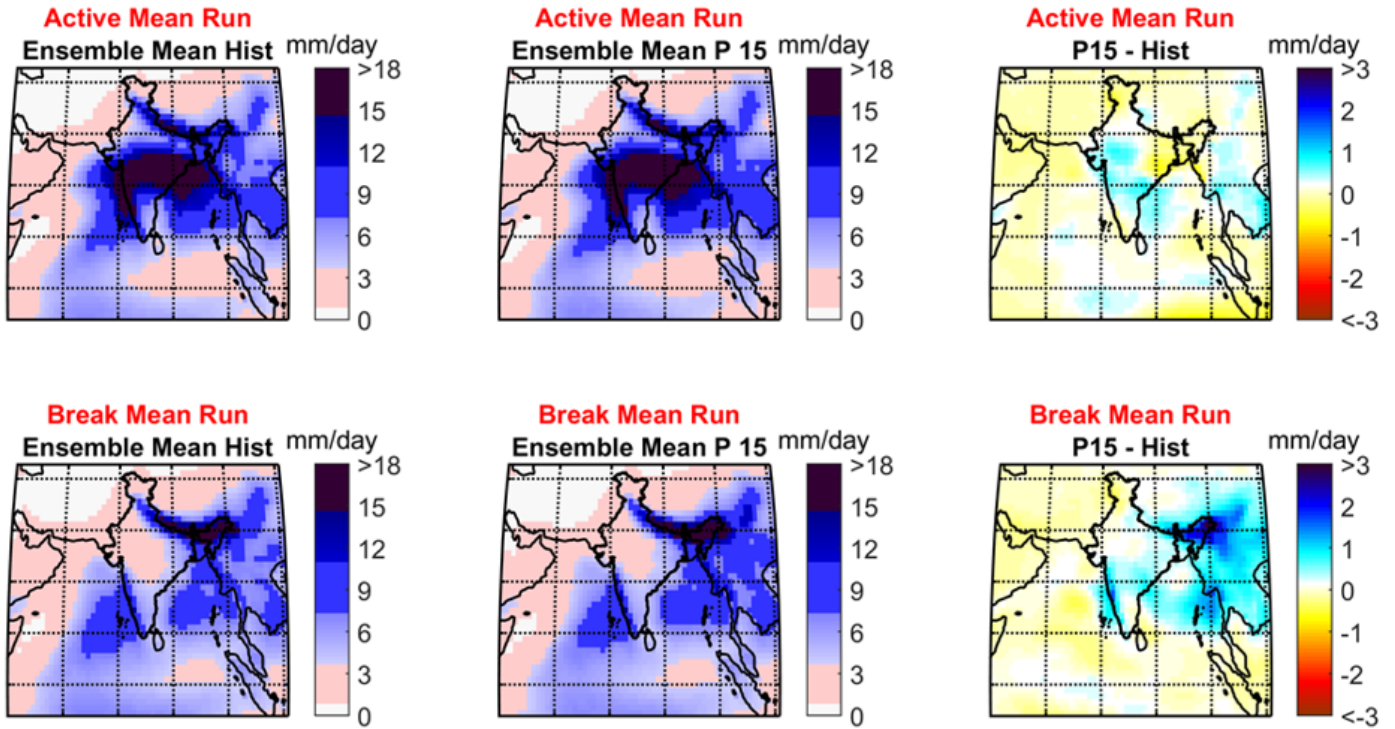


Figure 29

Ensemble mean of active and break period rainfall for historical and plus15 future period (1.5°C warming condition).

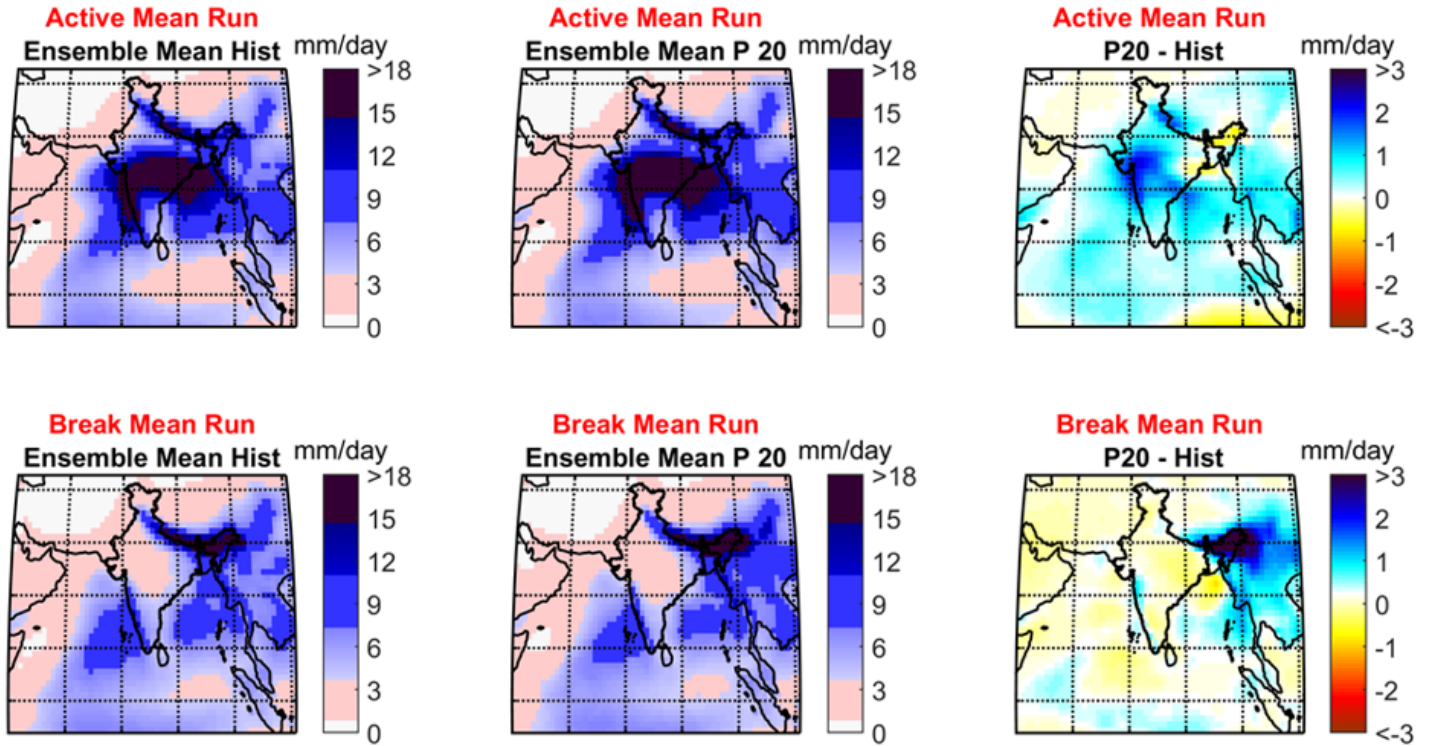


Figure 30

Ensemble mean of active and break period rainfall for historical and plus20 future period (2°C warming condition).

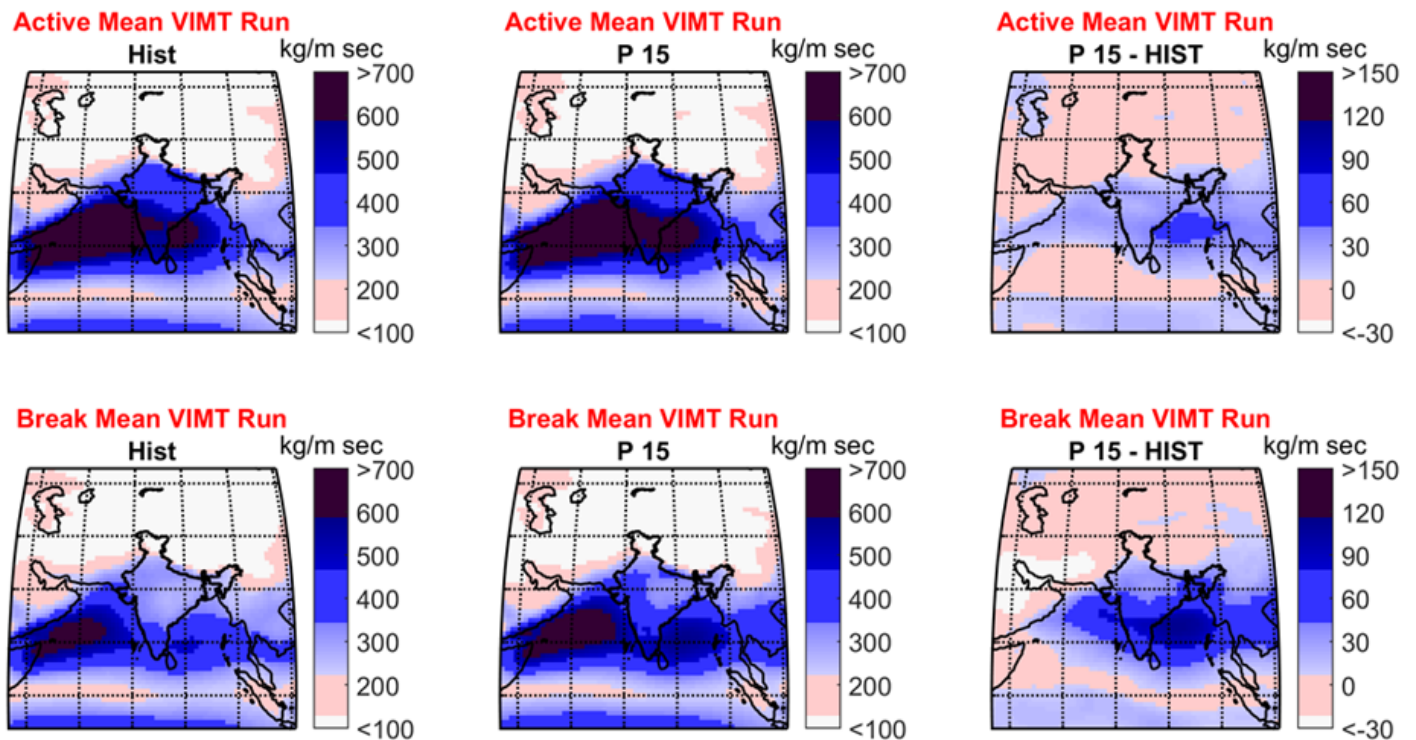


Figure 31

Active and break period VIMT (Vertically integrated moisture transport) of the *NorESM1* model for historical and plus15 period.

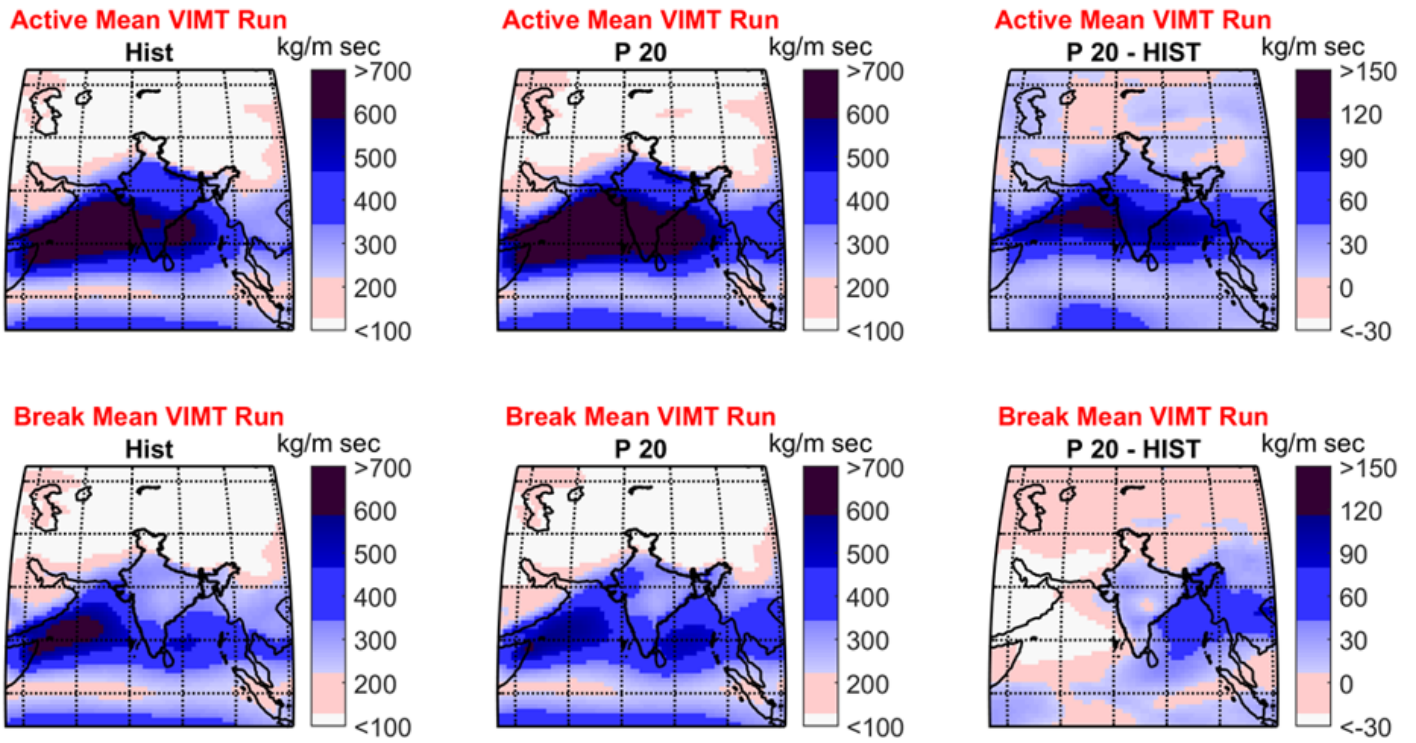


Figure 32

Active and break period VIMT (Vertically integrated moisture transport) of the *NorESM1* model for historical and plus20 period.